

QUARTZ VEIN INVESTIGATION, MCDOWELL SONORAN PRESERVE, SCOTTSDALE, MARICOPA COUNTY, ARIZONA

Brian F. Gootee¹ & Daniel G. Gruber²

¹Arizona Geological Survey | ²McDowell Sonoran Field Institute

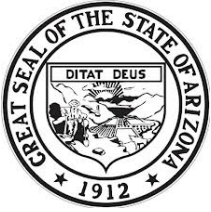


OPEN-FILE REPORT OFR-15-03

July 2015

Arizona Geological Survey

www.azgs.az.gov | repository.azgs.az.gov



Arizona Geological Survey

M. Lee Allison, State Geologist and Director

Manuscript approved for publication in July 2015

Printed by the Arizona Geological Survey

All rights reserved

For an electronic copy of this publication: www.repository.azgs.az.gov

Printed copies are on sale at the Arizona Experience Store

416 W. Congress, Tucson, AZ 85701 (520.770.3500)

For information on the mission, objectives or geologic products of the Arizona Geological Survey visit www.azgs.az.gov.

This publication was prepared by an agency of the State of Arizona. The State of Arizona, or any agency thereof, or any of their employees, makes no warranty, expressed or implied, or assumes any legal liability or responsibility for the accuracy, completeness, or usefulness of any information, apparatus, product, or process disclosed in this report. Any use of trade, product, or firm names in this publication is for descriptive purposes only and does not imply endorsement by the State of Arizona.

Recommended Citation: Gootee, B.F. and Gruber, D.G., 2015, Quartz vein investigation, McDowell Sonoran Preserve, Scottsdale, Maricopa County, Arizona. Arizona Geological Survey Open File Report, OFR-15-03, 69 p.

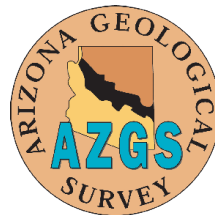


Table of Contents

Table of Contents	ii
List of Tables	iii
List of Appendices	iii
1.0 Introduction and Setting	4
1.1 <i>Previous Work</i>	4
1.2 <i>Methods and Site Selection</i>	4
1.2.1 Reconnaissance and Site Selection.....	4
1.2.2 Geologic Mapping.....	10
1.2.3 Aerial Balloon Photography.....	11
1.2.4 Rock Sample Analysis.....	13
2.0 Fraesfield Site	14
2.1 <i>Geologic mapping</i>	14
2.2 <i>Rock Sample Analysis and Interpretations</i>	20
2.2.1 Sample F1: Milky Quartz.....	20
2.2.2 Sample F2/F3: Mica-Quartz Schist.....	22
2.2.3 Sample F4: Banded Mylonite.....	25
2.2.4 Sample F5: Quartzite.....	27
2.2.1 Sample F6: Mica-Quartzite.....	28
2.2.1 Sample F7: Mica-Quartz Mylonite.....	30
2.3 <i>Summary and Conclusions</i>	32
3.0 Paraiso Site	34
3.1 <i>Geologic mapping</i>	34
3.1.1 Carefree Granite (Yg).....	34
3.1.2 Milky Quartz (Ymq).....	34
3.1.3 Pegmatite (Yp).....	35
3.2 <i>Rock Sample Analysis and Interpretations</i>	42
3.2.1 Sample P1: Graphic Granite.....	44
3.2.1 Sample P2: Gneiss or Mylonite.....	46
3.2.1 Sample P3: Orbicular Granite.....	47

3.2.1 Sample P4, P5 and P7: Milky Quartz 51

3.2.2 Sample P6: Fine-grained Granite 53

3.3 *Interpretations and Conclusions* 56

4.0 Implications and Next Steps 60

4.1 *Implications for and Applicability to Other Quartz Veins Outcrops* 60

4.2 *Additional Research Questions* 60

Acknowledgements 61

References Cited 62

Glossary of Geologic Terms 64

List of Tables

Table 1. Reconnaissance results and assessment for each quartz vein site. 8

Table 2. Results of the XRF spectroscopy analyzer used on Fraesfield samples. 21

Table 3. Results of the XRF spectroscopy analyzer used on Paraiso samples. 43

List of Appendices

- A. Agisoft Reports for Balloon Photography SfM Mapping at Fraesfield and Paraiso sites.
- B. Basic data for samples collected at the Fraesfield and Paraiso sites.

1.0 Introduction and Setting

1.1 Previous Work

Milky quartz veins are visible throughout all parts of Scottsdale's McDowell Sonoran Preserve (the Preserve) (see locator map below) and at many scales. Prospectors searching for heavy metal and mineral deposits have historically been attracted to milky quartz and represent the earliest researchers. Pits and tailings are occasionally found with milky quartz, however written records of mining activity are usually not found.

Quartz veins and large milky quartz deposits are commonly found in Proterozoic rocks throughout Arizona. Research targeted at milky quartz has not been done in the greater Phoenix area, and as such, little is known about their formation and emplacement history. Thus, previous works in the region and by topic were researched during our study. Karlstrom and others (1991) provided valuable context to the Fraesfield site. Jahns (1953) provided great insight into pegmatites in the White Picacho District, as they relate to pegmatites at Paraiso. Several other topical references, cited throughout this report, were used to help characterize both sites.

Early geologic mapping in the Fraesfield and Paraiso areas have generally noted the presence of milky quartz in association with its host rock and identified larger milky quartz bodies. Detailed geologic mapping in the area and region have provided important context and geologic setting crucial for studying quartz veins. Christensen and others (1978) conducted the first detailed map of the southern half of the McDowell Mountains. Péwé and others later mapped portions of northern Scottsdale and the Ft. McDowell area in 1983 (published 2012). Skotnicki and others mapped most portions of the Preserve area (Skotnicki, 1996; Skotnicki and others, 1997). Vance (2012) conducted detailed structural analysis and mapping of the McDowell Mountains as part of his MS thesis at Arizona State University. And most recently Steve Skotnicki has completed the most detailed and comprehensive mapping of the McDowell Mountains and its foothills (Skotnicki, 2014, unpublished).

1.2 Methods and Site Selection

1.2.1 Reconnaissance and Site Selection

Massive milky-quartz veins are exposed in the Preserve within Proterozoic bedrock. Many exposures of milky quartz features can be seen from or are found near trails. Although some of these features have been mapped relative to other geologic units by previous researchers (Christensen *et al.*, 1978; Couch, 1981; Skotnicki, 1986; Vance, 2012), little research has been done to determine their origin, emplacement history, and geochemistry (Gootee, 2012).

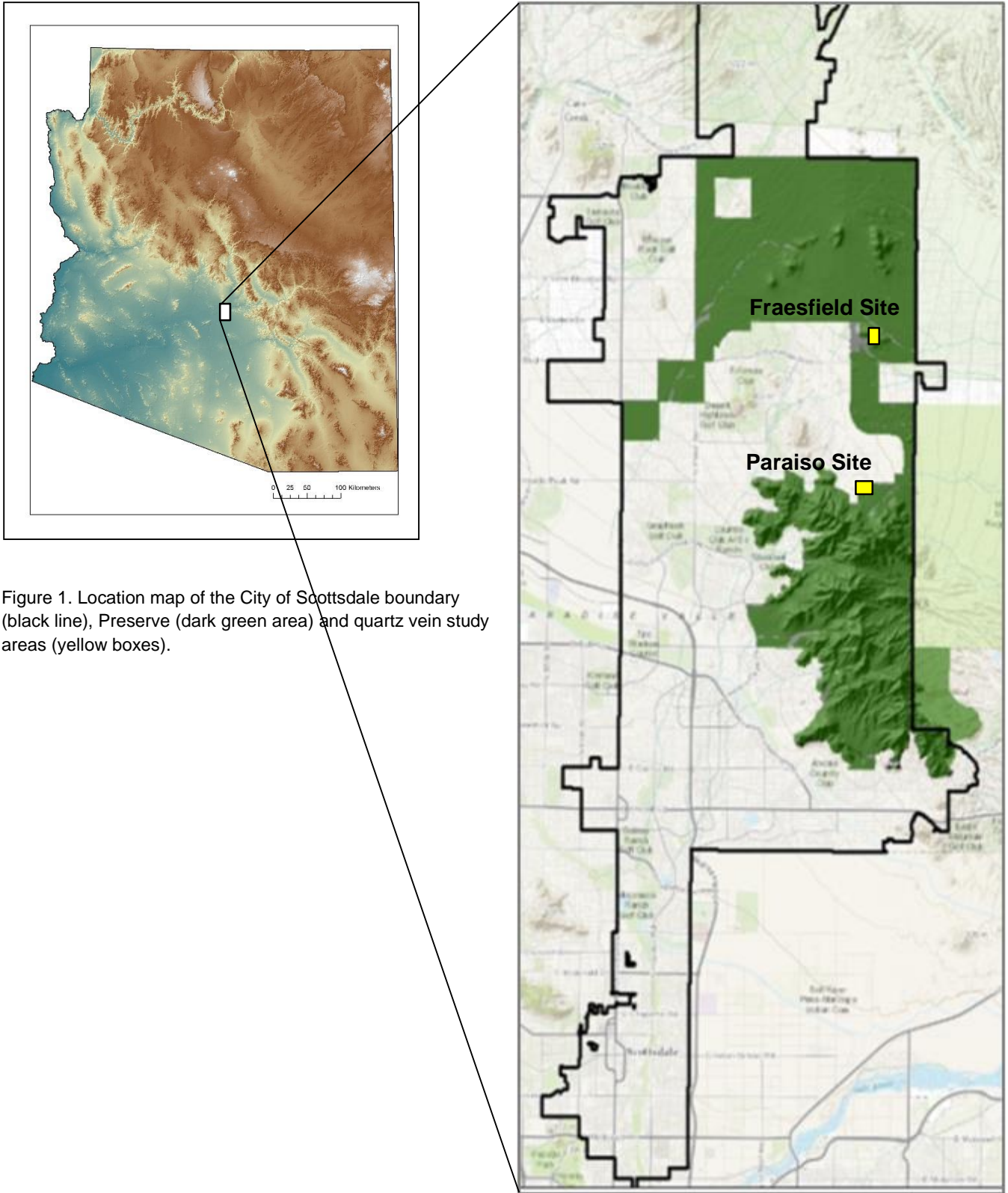


Figure 1. Location map of the City of Scottsdale boundary (black line), Preserve (dark green area) and quartz vein study areas (yellow boxes).

In order to research these aspects of the milky quartz deposits, the Arizona Geological Survey (AZGS) proposed to work in conjunction with the McDowell Sonoran Field Institute (MSFI), the research center of the McDowell Sonoran Conservancy (MSC), to develop detailed maps of several individual quartz bodies. The proposal included four basic tasks:

1. Locate and evaluate prominent milky quartz deposits in the Preserve to choose candidates for research.
2. Select research sites and describe them in detail (“micro-mapping”) with associated measurements, observations, and possible sampling.
3. Produce maps of the sites, review the collected data, and analyze any samples.
4. Prepare a summary report.

The first task, choosing candidates for detailed study, consisted of several steps. First, trained MSFI volunteers using Google Earth (GE) performed a detailed aerial survey of the entire Preserve area. A basic GE view was created that divided the Preserve into twenty areas of approximately equal size, with known quartz bodies identified (See Figure 2).

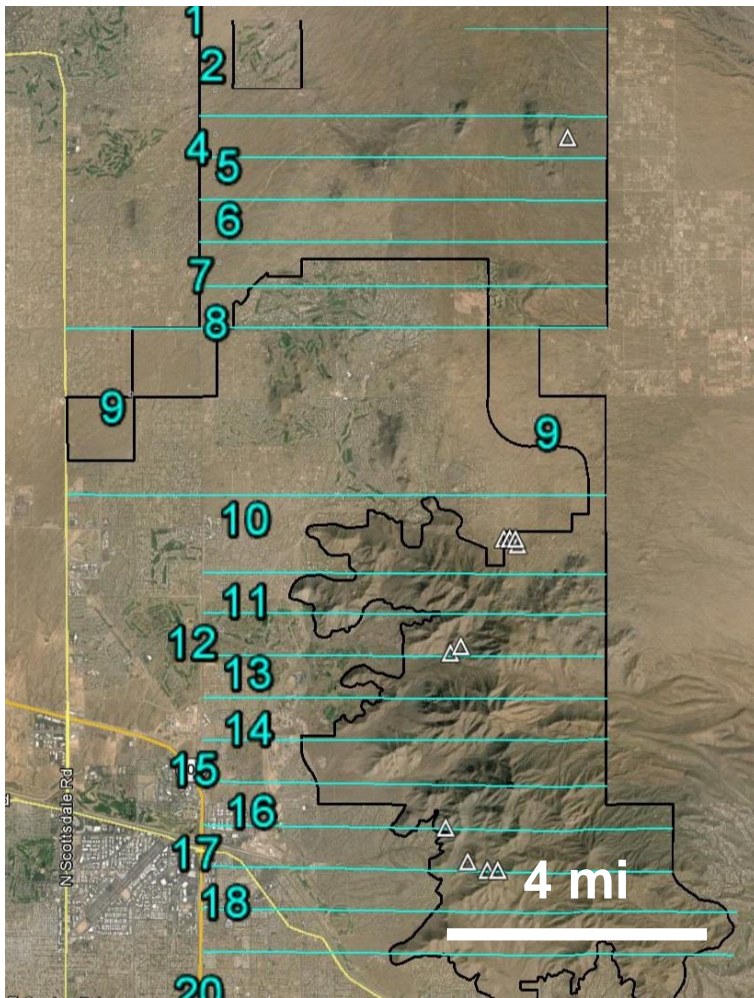


Figure 2. Aerial view from Google Earth showing scan setup (numbered blue lines) and quartz vein candidate sites (white triangles). Preserve boundary shown in black. North to top.

Volunteers visually inspected each area on GE and recorded possible quartz outcrops on a worksheet. The project leader then visually reviewed each recorded candidate on GE. This process revealed several possible milky quartz outcrops not previously mapped (see Additional Research Questions). Principal Investigator (PI) Brian Gootee, research geologist with AZGS, reviewed potential candidates and selected nine sites for preliminary field reconnaissance.

MSFI volunteer teams led by the project leader and usually the PI visited the nine sites. For most of the sites, reconnaissance mapping delineated the orientation of major features in the outcrop(s) and the teams recorded basic measurements, photos, and field observations. The PI developed criteria to help assess and rank each site, which were applied to the field reconnaissance results. Table 1 shows the assessment results. Note that two sites are not shown in the table. One site (Silverleaf) was outside of the Preserve on private property. The other site (Sunrise) proved not to be a quartz vein.

Table 1. Reconnaissance results and assessment for each quartz vein site.

Assessment Criteria	1 Quartz Trail*	2 Tom's Thumb Complex* ¹	3 Paraiso Complex* ¹	4 Fraesfield Complex	5 Paradise Mine ¹	6 Prospector Complex ¹	7 Troon Complex
Measurable feature?	Y	Y	Y	Y	Y	Y	N
Bedrock contacts on one side/both sides of outcrop?	both?	one	both	one	both	both	one
Variations within the main quartz body?	Y	?	Y	Y	Y	Y	Y
Mineralization or cavities on the surface of the quartz body?	Y	?	Y	?	N	Y	Y
Bedrock in vicinity of outcrop in one direction/both directions?	both?	?	?	both	both	N?	both
Foliation in nearby rock in one direction/both directions?	one?	?	N?	both	one	both	N
Significant changes in the character of nearby rock?	Y	?	N?	Y	Y	N	N
Quartz veins in nearby bedrock or boulders?	Y	?	N?	Y	Y	N	Y
Other notable features? Describe:	One unit with lots of black mineralization	Multi-unit, linear feature with one side buried in colluvium	Large group of cylindrical plugs, different from all other sites, extensive tourmaline and brightly-colored minerals	Several widely-spaced units in middle of shear zone surrounded by bedrock	Multi-unit, main unit curved, highly fractured bedrock nearby	Multi-unit, copper in debris, near mine tailings pile	Single small quartz unit in extensive quartzite outcrops
Overall assessment?	M/H	L	H	H	M	M	L

* No written notes

¹ Multiple units; assessment applies to some/all units

? Indicates uncertainty

The PI selected the Paraiso and Fraesfield sites (sites 3 and 4) for detailed micro-mapping and analysis as a result of this assessment process. These two sites are in different geological settings but the basic methods and approach were similar for both sites (Pictures of each site are shown in Figure 3 and Figure 4).

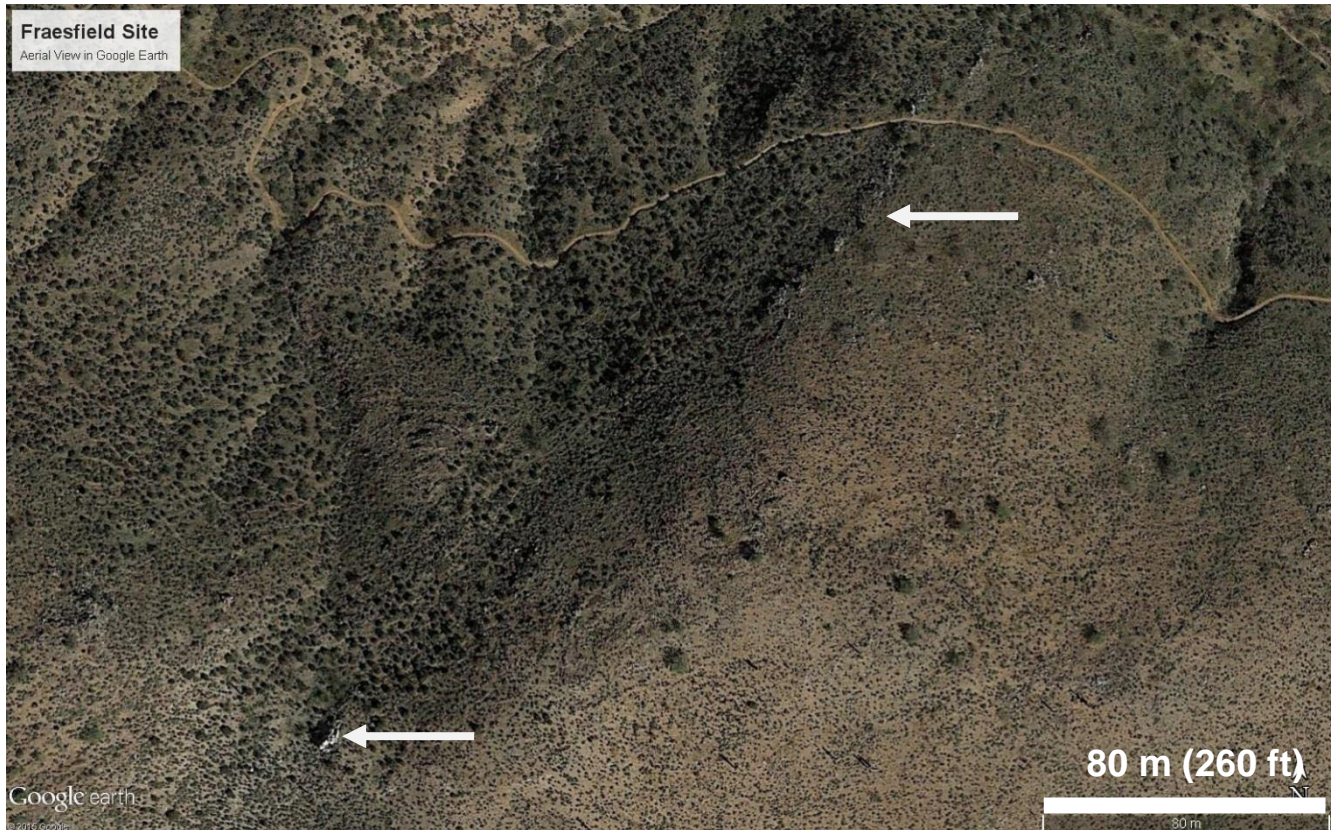


Figure 3. Aerial view from Google Earth of the Fraesfield site. The milky quartz outcrops and related features are visible in a lineament from lower left center to upper right center (arrows). North to top.

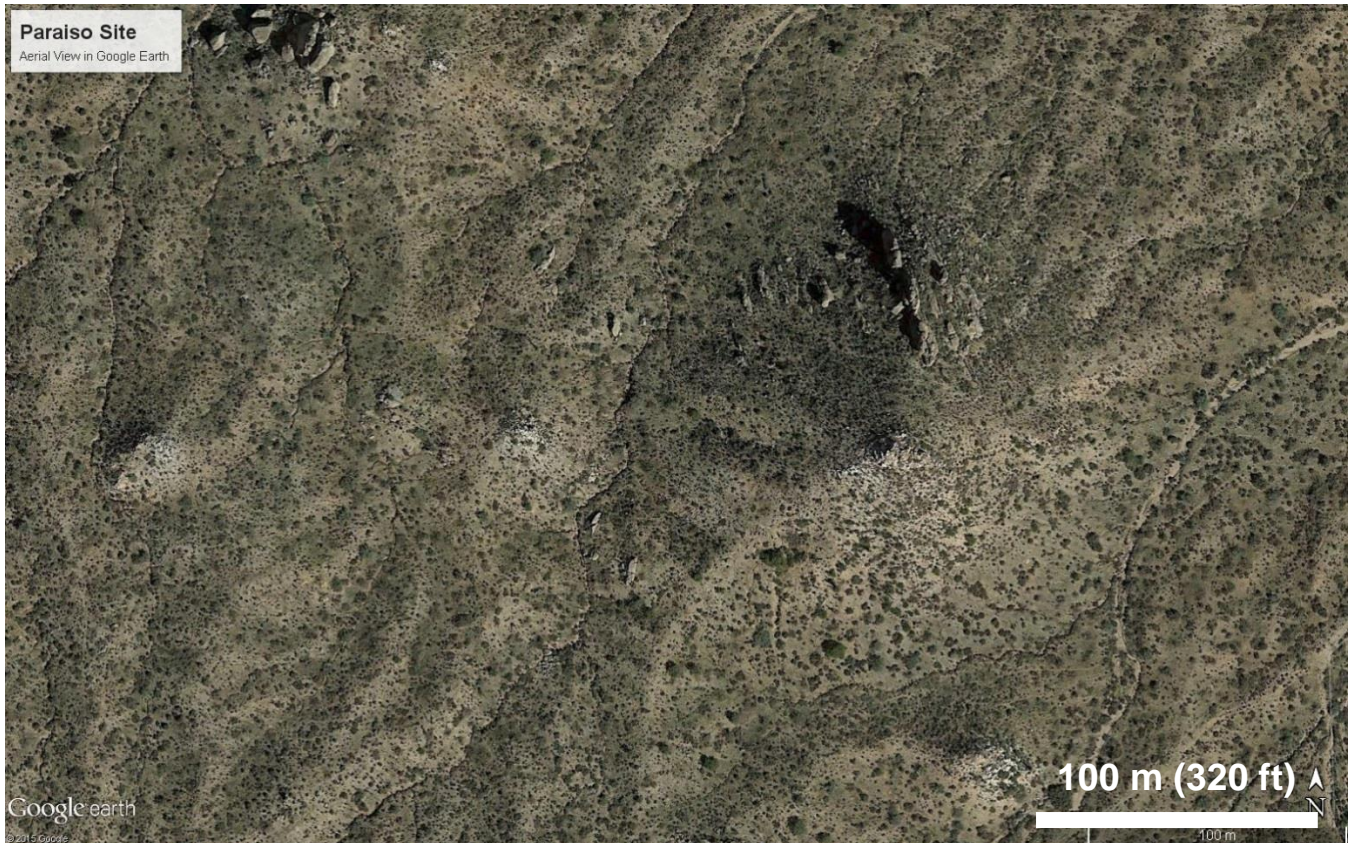


Figure 4. Aerial view from Google Earth of the Paraiso site. The many quartz outcrops are in light-colored circular areas. North to top.

1.2.2 Geologic Mapping

The purpose of mapping at both context and core scales was to map the extent, structure and relationships between rock types and geologic units that encapsulated several milky quartz features. Mapping the composition and distribution of specific mineral or mineral groups/associations, especially in the milky quartz zones, was beyond the scope of this effort.

First, the PI demarcated core and context areas for each site. The core areas (1 – 2 hectares) were mapped in detail, while only major features were mapped in the context areas (5 – 10 hectares). Field mapping was done almost entirely by trained volunteers under the supervision of the project leader, with field checking performed periodically by the PI. Field maps were drawn on vellum overlays over 10 cm/pixel aerial imagery provided for each research site by the City of Scottsdale GIS department. (Figure 5 to Figure 8 show the core area maps on vellum and the core area field map overlays.) Relevant geologic data were recorded on separate worksheets and basic data plus GPS waypoints noted on the field maps.



Figure 5. Fraesfield Core Area vellum overlay.



Figure 7. Fraesfield Core Area aerial imagery with vellum.

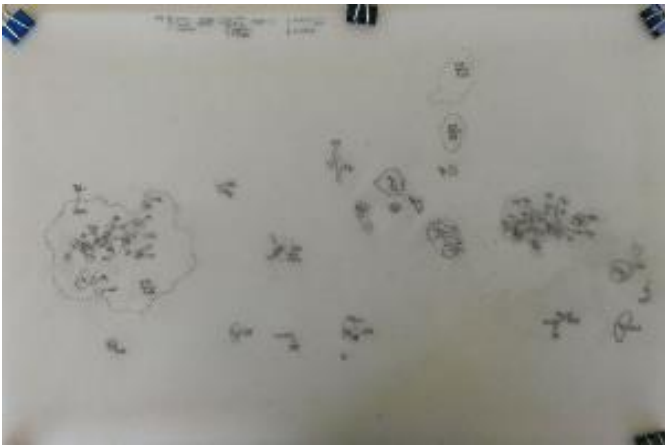


Figure 6. Paraiso Core Area vellum overlay.



Figure 8. Paraiso Core Area aerial imagery with vellum.

After final field checking by the project leader and the PI, the four vellum field maps (Paraiso core and context, Fraesfield core and context) were georeferenced onto the MSFI base map for the Preserve in ArcMap. Trained volunteers then traced the georeferenced field overlays in ArcMap, with topology checked by the PI and corrected by the project leader. Point data were entered into Excel worksheets and imported into ArcMap. The resulting digital linework and point data were used by the PI to create the four survey maps discussed in the Fraesfield and Paraiso sections below.

1.2.3 Aerial Balloon Photography

At each site, a tethered helium-filled weather balloon was used to loft a downward-pointing digital camera (Figure 9). This apparatus, lent to the project by Professor Ramon Arrowsmith of Arizona State University (ASU), was carried in a grid pattern across the sites, with the balloon and camera tethered at 50 meters over the core areas and at 100 and 150 meters over the larger context areas. The camera aperture was such that each aerial photo covered an area approximately the same width as the elevation of the camera, and the grid pattern used to pull the tethered balloon over each area was designed to produce 50% overlap of adjacent passes. The camera automatically took high-resolution (10 megapixel) photos every 10 seconds, corresponding to 5 – 15 meter intervals depending on terrain.

This process produced hundreds of overlapping digital photos of each area taken from varying elevations and at varying angles due to wind effects on the balloon and suspended camera. The photos were uploaded into Agisoft Photoscan, a software package that generates three-dimensional spatial data from digital images using a technique called Structure from Motion (SfM). SfM processing does not require advance specification of camera position or the location of ground control points. Instead, the technique automatically identifies matching features in multiple images and refines their relative positions as they appear in more images. After SfM processing, the resulting image and digital elevation model (DEM) are georeferenced to real-world coordinates by identifying and providing coordinates for obvious ground features in the image that serve as ground control points.

Initial field mapping work was done on vellum placed over 10 cm/pixel aerial photographs provided by the City of Scottsdale. However, the four survey maps (core and context area maps for the Fraesfield and Paraiso sites) use georeferenced SfM-generated aerial photographs as base layers and SfM DEMs to calculate contour lines. Topographic accuracy and aerial photography resolution are estimated by the Agisoft software. At these sites, the former was estimated as ~2 cm and the latter at ~4 to 5 cm/pixel. A summary of SfM results and byproducts is provided in Appendix A.



Figure 9. Brian Gootee with ASU's helium-filled balloon used to conduct the aerial survey.

1.2.4 Rock Sample Analysis

Once geologic mapping was completed, rock samples were collected for thin-section analysis. A thin section is a thin slice of rock sample shaved down to 0.03 millimeters (30 microns), or about the thickness of a tissue. The orientation of each sample was labeled in order to determine the orientation of micro-structures in thin section, such as sense of shear. Each thin section was assigned a geologic unit from which it was collected and referenced to the geologic map. Each thin section was carefully studied to identify its texture, mineral type and abundance (including opaque, cubic, accessory, trace and retrograde minerals), deformation texture, and any other notable features. Sample IDs were later relabeled with a prefix site letter (F for Fraesfield, P for Paraiso), the nomenclature used herein.

Samples of milky quartz were also collected from each site for fluid inclusion analysis. During the growth of minerals, fluids can be trapped within mineral grains. Fluid inclusions trapped in minerals can be extracted and can provide information about changing fluid temperature and salinities associated with mineralogical changes, which can clarify vein evolution and perhaps magmatic and groundwater influences on hydrothermal fluid characteristics. Oxygen isotopes of hydrothermal minerals can clarify the role of magmatic and meteoric waters in vein growth. Thin sections for fluid inclusion analysis in quartz were cut three times thicker (90 microns) than a normal thin section (30 microns) and did not include cover slips on the thin section. An immersion oil with the same refractive index as the quartz is poured on the sample, which fills any pits on the surface. This allows for a three-dimensional view into the quartz, which is necessary to study internal fluid-inclusions under a petrographic microscope.

Thin sections were analyzed using a special microscope called a petrographic microscope (petroscope), which allows polarized light to be transmitted from the base of the scope up through the thin section and to the observer. This method allows the geologist to identify microscopic mineral composition, texture and structure. A Leitz Wetzlar Dialux-Pol from the AZGS Tucson office was used to analyze thin sections. Due to problems encountered with the petroscope the identification of minerals under high power (such as optical character) was difficult or in some cases not possible. Thus mineralogy of samples was predominantly done using more qualitative characteristics.

Prior to cutting the samples for thin sections, the hand samples were analyzed with field instruments from the AZGS Phoenix office including a shortwave ultraviolet (UV) lamp, Geiger counter, and portable x-ray fluorescence (XRF) spectrometer. UV light is used to identify the presence of minerals and/or impurities in minerals that fluoresce when exposed to such light. A Geiger counter is used to detect and measure the presence of ionizing radiation due to radiogenic minerals such as uranium and thorium present in a rock. The XRF analyzer emits x-rays ~3/8-inch into a sample, which results in chemical-element fluorescence and emission of diagnostic x-rays that are identified by the detector. This allows certain metal elements such as copper, gold, magnesium, etc. to be detected in relevant quantities in the rock sample. In comparison to laboratory methods, this method has low precision but allows field examination of many more samples. Only 25 elements, mostly metals, are capable of being detected by the AZGS XRF Analyzer (Thermo Niton XLt Portable XRF Analyzer).

2.0 Fraesfield Site

2.1 Geologic mapping

Reconnaissance mapping of the Fraesfield quartz vein site was conducted for context and detailed core areas. Methods for site selection and subsequent geologic mapping are described in Section 1.2.2. The results of mapping are shown in one small-scale context map with legend (Figure 13) and one large-scale core map (Figure 14). Each geologic unit is described in Figure 13. Strike and dip of foliation and bedding in quartzite are plotted in both maps.

The majority of geology at Fraesfield is characterized as loose unconsolidated colluvium that covers complexly-related quartzite, granite and foliated bedrock. In order to characterize the context of milky quartz and surrounding bedrock, colluvium rich in one bedrock type was mapped differently from colluvium dominated by another type or suite of constituents. This approach was used in order to determine the relationships between quartz veins and granite/quartzite bedrock. Through geologic mapping we discovered that all bedrock units along the margin of mica-schist were non-sheared bedrock that grades laterally into sheared bedrock, with increasing shearing intensities towards strongly foliated and mylonitized mica-schist. Thus, the milky quartz vein is embedded in a foliated and mylonitized shear zone that strikes northeast-southwest through the study area.

The milky quartz at Fraesfield is characteristic of many other milky quartz deposits in the Preserve and the region, which are typically found along bedding and foliation planes in Proterozoic rocks, predominantly metamorphic rocks. The Fraesfield milky quartz is massive, light gray-white weathered to wispy-white on fresh unweathered surfaces. The quartz does not appear to have cavities or obvious zoning or layering, but upon close inspection with a hand lens faint fine laminae are visible (not visible in Figure 10). Many other quartz veins subparallel to parallel to foliated schist were observed. Quartz veins typically bulge near their center and have tapered or lenticular ends. Nearly all quartz veins appeared to be deformed within the shear zone, although some veins were parallel to foliation and lacked deformation. Quartz veins were not observed cutting across foliated schist.



Figure 10. Sample F1, an oriented sample of milky quartz at Fraesfield.

The oldest unit in the study area is quartzite. This unit is believed to be approximately 1,600 million years (Ma), i.e., Paleoproterzoic (Skotnicki, 1996; Skotnicki et al., 1997); however, recent mapping by Skotnicki (2014) may provide a slightly different age. Cross-bedding is remarkably well preserved in non-foliated portions of this unit, outlined by thin laminae of magnetite (Figure 11). Both planar and trough cross-beds are preserved in quartzite and indicate a top-to-the-northwest orientation west of the shear zone and top-to-the southeast east of the shear zone. Skotnicki et al. (1997) reported that the stratigraphic top direction was to the southeast. The contrast in bedding orientations may indicate overturned bedding. Thin to medium non-deformed veins of milky quartz were observed cross-cutting quartzite bedding (captured in Sample F6). Two exposures of quartzite - in the far southeastern context map area, and in the northwest area immediately north of the core mapping area (Figure 13) - are believed to be xenoliths surrounded entirely by granite. Detailed mapping of surrounding granite, degree of metamorphism and contrast in bedding orientations support this idea.



Figure 11. Sample F5 was collected from this outcrop, a cross-bedded sand outlined by thin laminae of dark magnetite bands, indicating bedding is upright with tops-to-the-northeast (upper right in photo).

A coarse-grained granite is present in the mapping area, has inclusions of quartzite within it, and intrudes quartzite. The age of granite is uncertain but believed to be similar to the Carefree granite, ~1,425 Ma (Isachsen and others, 1999). Quartz veins were not observed cross-cutting granite or emanating from granite into quartzite, albeit there is a lack of abundant exposures.

The shear zone cross-cuts granite and quartzite and consists of a fine-grained foliated to mylonitized mica-schist. Degree of foliation varies from strongly foliated to ultra-mylonitic. Although quartz veins are mildly to heavily deformed and folded along their margins, quartz veins represent the most competent rock type in the shear zone. Margins of quartz veins in the shear zone also appeared to be interleaved with mica, where more semi-brittle and ductile deformation fabrics were observed, such as folds and kink-banding (Figure 12). Margins of the shear zone varied from sharp over a few centimeters to gradational over a few meters into competent bedrock. Slivers and blocks of non-foliated quartzite and granite were observed along the shear zone margin. Based on cataclastic textures, increasing degrees of sheared textures, and a mechanical reduction of grain size in the granite along the shear zone, we interpret shearing to post-date emplacement of the granite. Alternatively, shearing from magmatic emplacement can also occur (Nyman et al., 1994), although textures unique to magmatic shearing are not consistent with those observed at Fraesfield.

The general shear-zone strike is to the northeast, dipping 65 to 75 degrees to the southeast. Analysis of thin sections from samples F2, F4 and F7 indicate a sinistral or left-lateral sense of movement (east side to the northeast). The amount of offset is unknown. The strike and sense of this shear zone coincides with other mylonite shear zones in the Preserve (Skotnicki, 2015, personal communication). This shear zone also coincides with the northeast-striking Slate Creek shear zone in the Mazatzal Mountains area east of Bartlett Dam (Wessels and Karlstrom, 1991). The age of shearing

is not certain but obviously is post 1,425 Ma, possibly related to the Grenville Orogeny circa 1,200 to 1,100 Ma (Skotnicki, 2015, personal communication).



Figure 12. Foliated, folded and kink-banded milky quartz vein. Note micaceous portions are heavily weathered and not apparent in outcrop. Pencil defines trend and dip of a fold axis. View to southeast.

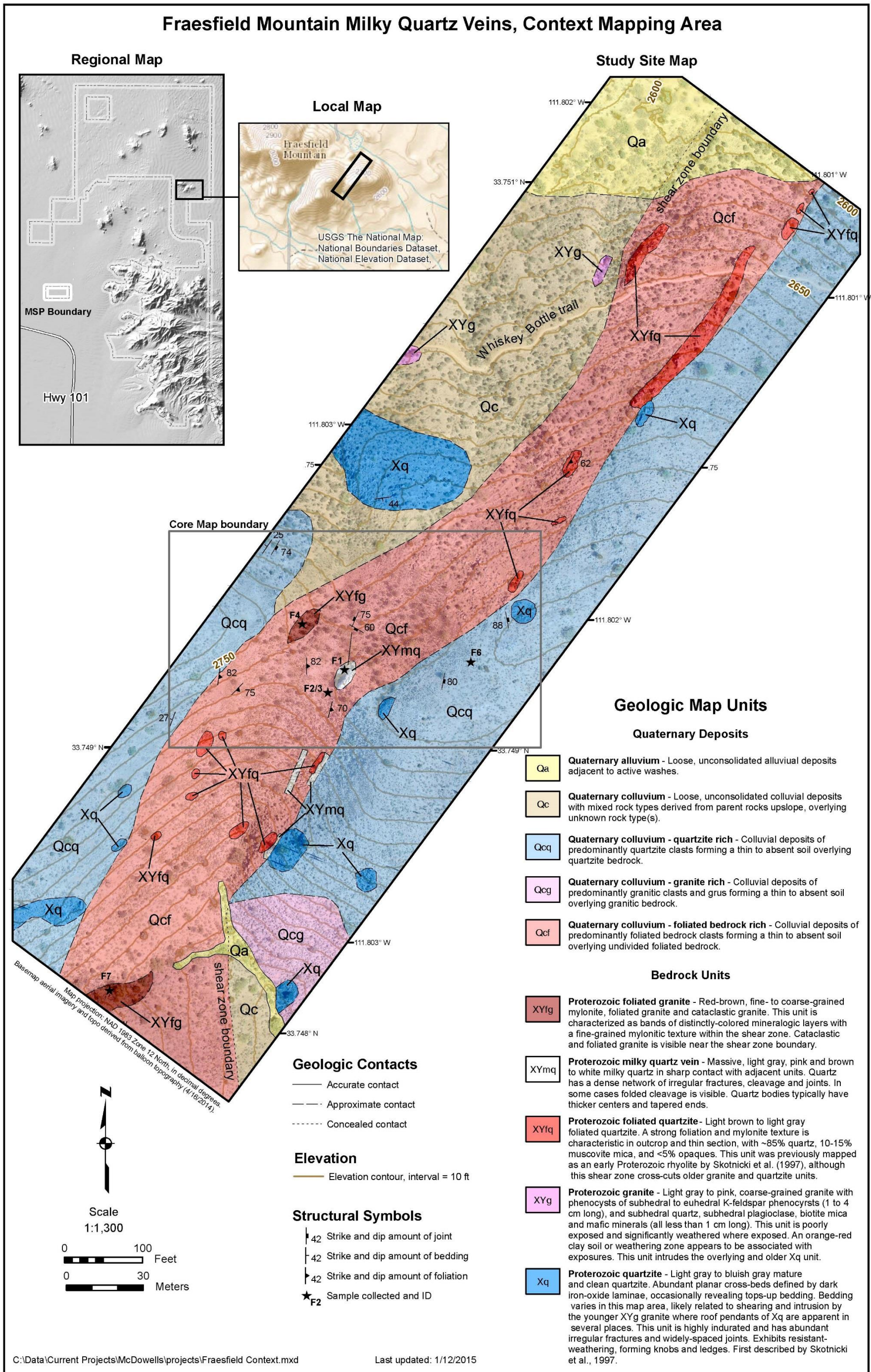


Figure 13. Fraesfield context geologic map.

Fraesfield Mountain Milky Quartz Vein, Core Mapping Area

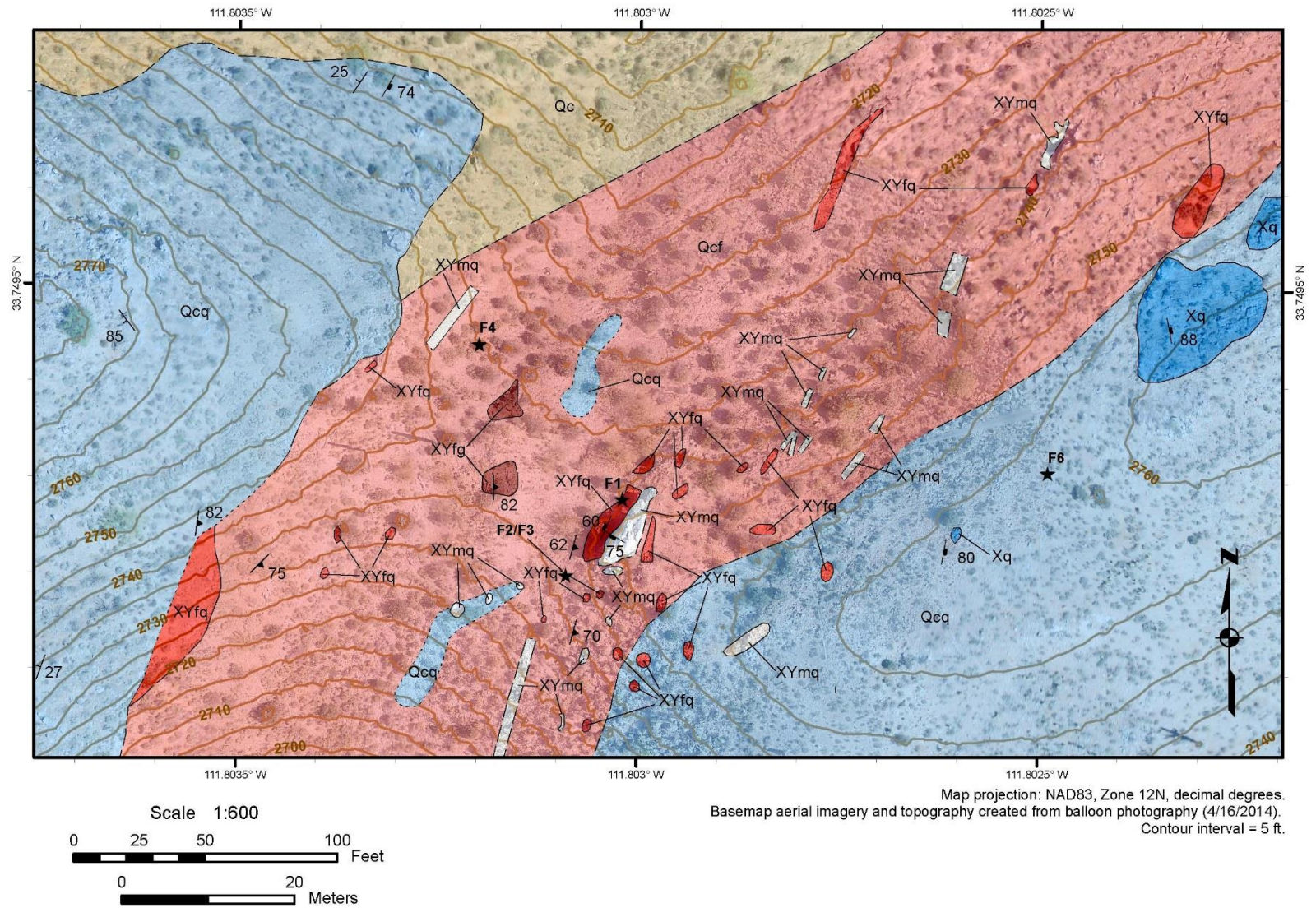


Figure 14. Fraesfield core geologic map. See context geologic map in Figure 13 for explanation of units and extent of map.

2.2 Rock Sample Analysis and Interpretations

Once geologic mapping was nearly complete, six samples were collected at the Fraesfield site. Samples F1 to F4, and F6 are plotted on the Fraesfield geologic map (Figure 13). Sample F5 was collected from non-deformed quartzite a few 10's of meters west of the context map area. Basic data for all samples are listed in Appendix B. One sample from the massive milky quartz vein was submitted to Jim Reynolds of Fluid Inc. to evaluate the existence and condition of fluid inclusions preserved in quartz. The remaining samples were cut for thin section. Two thin sections made for each foliated rock sample, one parallel and one perpendicular to the foliation plane. X-Ray fluorescence (XRF) analyzer results for Fraesfield samples are listed in Table 2.

2.2.1 Sample F1: Milky Quartz

Sample F1 Observations

This sample was collected from the main milky quartz deposit in the study area (Figure 10). The quartz is milky white to semi-transparent, very finely layered with abundant micro-fractures and densely-spaced joints. Analysis for fluid inclusions by Jim Reynolds characterized the quartz as having trillions of micron-sized fluid inclusions on billions of microfractures resulting in a texture commonly referred to as "bull quartz". A photomicrograph at lower power reveals the laminated and very fine-grained texture of milky quartz at this site (Figure 15). Also associated with this milky quartz are wispy microfractures, decrepitation texture, transposed planes and double-bubble textures, commonly associated with bull quartz. At 50x magnification inclusions are not visible.

Due to the very fine-grained size of quartz grains, inclusions, and associated textures, a quantitative analysis of fluid inclusions could not be done. A minor percentage of opaque minerals (typically oxide minerals) is seen lining fractures. In outcrop view this sample has dark gray to black deposits - likely algae - filling fractures exposed to the environment (Figure 10). Orange-brown oxide clays coat many fractures near the surface as well and are likely wind-blown dust that percolates along fractures to form a clay coating (Figure 10). Elements antimony and tin were detected in relatively high amounts at 321 ± 113 parts per million (ppm), and 195 ± 114 ppm, respectively (Table 2). Antimony may indicate the presence of stibnite (Sb_2S_3), a sulfide ore mineral. Tin may indicate the presence of the mineral cassiterite (SnO_2).

Table 2. Results of the XRF spectroscopy analyzer used on Fraesfield samples.

Sample and Elements. Concentrations in parts per million (ppm)	Fraesfield						
	F1: milky quartz	F2/F3: mica schist	F4: mylonite	F5: quartzite	F6: quartzite	F6: quartz vein	F7: mylonite
Strontium (Sr)	--	--	31 ± 6	--	25 ± 7	14 ± 3	49 ± 9
Rubidium (Rb)	--	55 ± 8	43 ± 6	6.3 ± 3.8	37 ± 8	12 ± 3	145 ± 14
Lead (Pb)	--	--	--	--	--	--	21 ± 14
Zinc (Zn)	--	--	--	--	--	--	48 ± 27
Copper (Cu)	--	--	37 ± 23	--	--	28 ± 15	--
Iron (Fe)	--	6,307 ± 304	6,954 ± 289	6,585 ± 301	3,640 ± 268	1,026 ± 86	50,300 ± 1000
Manganese (Mn)	--	--	172 ± 77	--	--	--	--
Chromium (Cr)	--	--	--	--	--	--	--
Antimony (Sb)	321 ± 113	183 ± 96	228 ± 88	--	--	208 ± 62	--
Tin (Sn)	195 ± 114	--	158 ± 89	--	--	171 ± 63	--
Cadmium (Cd)	--	--	--	--	--	67 ± 40	--
Uranium (U)	--	--	--	--	--	--	--
Nickle (Ni)	--	--	--	--	--	--	--
Mercury (Hg)	--	--	--	--	--	--	--
Silver (Ag)	--	--	--	--	--	--	--
Arsenic (As)	--	--	--	9.6 ± 6.2	--	--	--
Gold (Au), Cobalt (Co), Platinum (Pt), Zinc (Zn)	--	--	--	--	--	--	--

-- = may be present in low concentrations, but non-detected in XRF

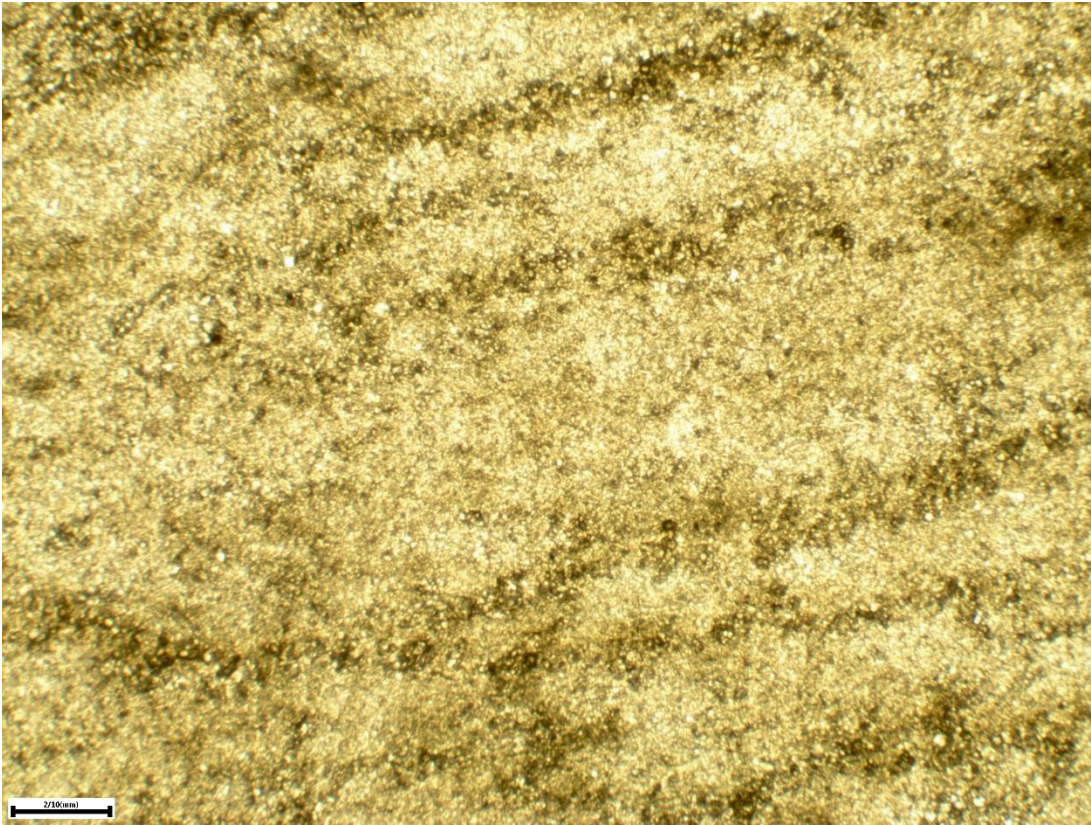


Figure 15. Sample F1 photomicrograph of milky quartz showing crude layering and individual very fine-grained quartz crystals smaller than 0.01 mm (10 microns). Scale in lower left equals 0.2 mm.

Sample F1 Interpretations

Based on field observations, the original milky quartz formed during or shortly after metamorphism of sandstone into quartzite, yet prior to shearing. Growth of milky quartz in this sample could not be related to the timing of the granite intrusion. In thin section the abundance of microfractures, multiple transposed planes of fractures, and inclusions (mineral and fluid) along fractures all suggest the bulk of milky quartz recrystallized during multiple episodes of quartz growth prior to, during and after deformation. Decrepitation textures that formed from exploding inclusions caused by heating by nearby magma sources or from burial or uplift paths indicate high temperature and/or moderate depths. The depth and temperature at which the milky quartz formed remains elusive. Antimony and tin ore minerals may be present, which may indicate significant (?) circulation of fluids through fractures and permeable zones such as the shear zone. In outcrop, wispy microfractures combined with countless microscopic fluid inclusions result in the milky quartz appearance.

2.2.2 Sample F2/F3: Mica-Quartz Schist

Sample F2/F3 Observations

Sample F2/F3 was collected from strongly foliated mica-schist within the shear zone (Figure 13). Two thin-sections were made, one perpendicular (F2) and parallel (F3) to foliation. The sample weathers to a light red-gray-brown color, and has a light green-white-gray color unweathered on a

freshly cut surface. Sample F2/F3 consists of 85 to 90% quartz and 10 to 15% mica with 1 to 2% opaque minerals. Several grains of sphene and/or zircon accessory minerals were observed (Figure 16). Opaque minerals could not be identified but appear to have formed with the original rock, and during or following two or three subsequent deformation events. The schist is strongly foliated and exhibits minor crenulation cleavage, asymmetric folds and kink-band folds. Quartz grains are moderate to highly reoriented in the plane of foliation, an indication of the degree of foliation. A quartz wedge was used to highlight how closely the c-axes of quartz crystals were aligned, shown by the equal-coloring of quartz grains (normally a quartzose sandstone would show randomly oriented crystallographic axes in thin section, and thus a random sampling of color hues) (See Figure 17).

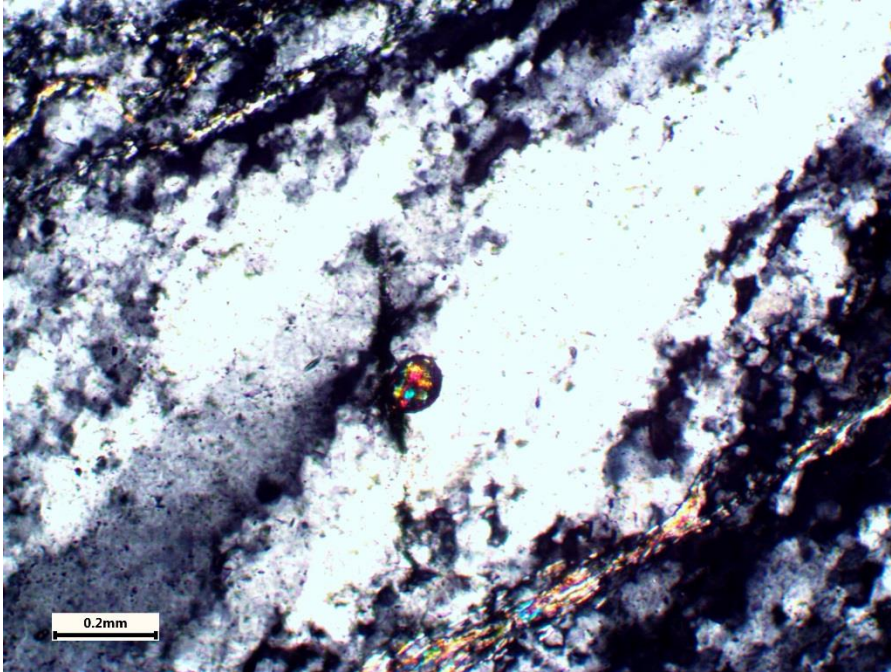


Figure 16. Sample F1 showing a single rounded zircon grain in a mass of recrystallized quartz. Scale in bottom left is 0.2 mm wide.

Quartz grain boundaries exhibit serrated sutures and possibly stylolites (Figure 18), which indicate dynamic recrystallization or boundary-migration recrystallization. Foliation exhibits a minor (?) amount of crenulation cleavage oblique to the plane of foliation, which is very difficult to see in hand sample. Both left- and right-lateral sense of shear was observed from mica “fish” in this sample. Some blocks of foliated textures were dislocated and brittle-deformed subsequently, and overgrown by equant, non-deformed quartz. A minor amount of very fine-grained mica and/or chlorite were observed as inclusions in quartz grains. XRF analysis detected relatively minor amounts of antimony in the sample (Table 2).

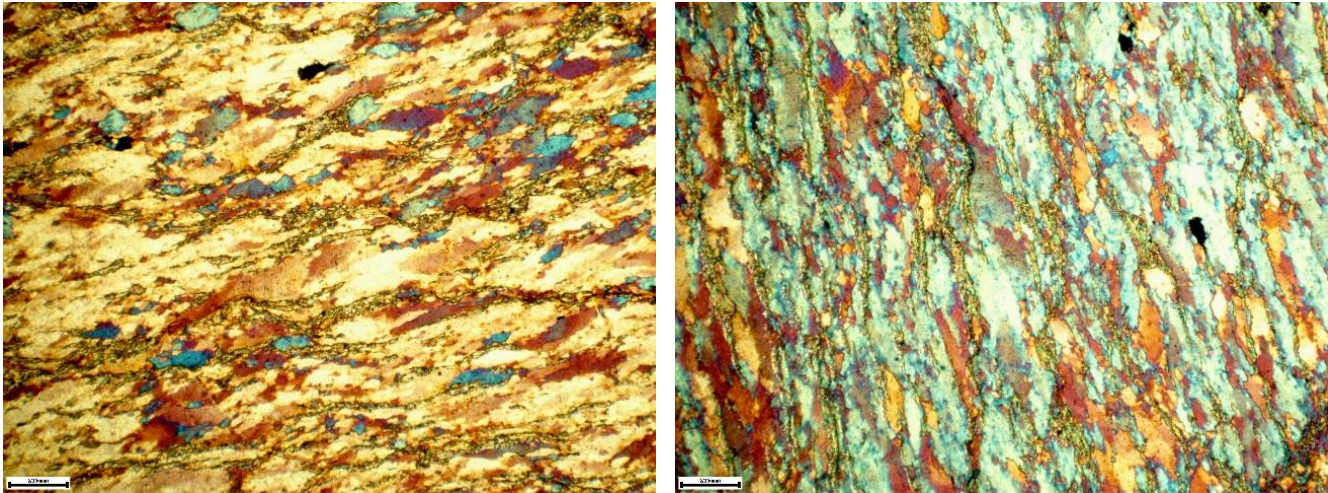


Figure 17. Sample F2 shown in cross-polarized with 95% quartz content at a low angle (left, and rotated 90 degrees (right). The similarity in yellow and blue hues show the degree of aligned quartz grains, an indication of the degree of foliation. Scale bar in lower left is 0.2 mm wide.

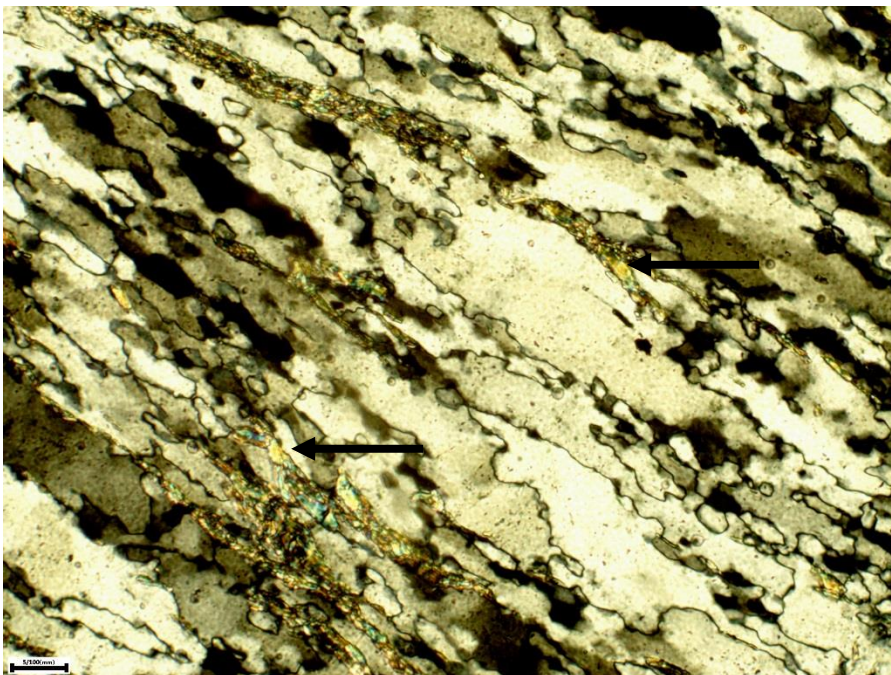


Figure 18. Sample F2 showing sutured and serrated quartz grain boundaries perpendicular to foliation. Colorful "fish" are mica minerals indicating the sense of shear (black arrows). Scale bar in bottom left is 0.05 mm (50 microns) wide.

Sample F2/F3 Interpretations

Based on the high quartz content and relationships with adjacent bedrock units observed during mapping, rounded zircon grains, and the lack of feldspar, the mica-quartz schist is interpreted to have originally been quartzite prior to shearing. The sandstone protolith probably was deposited between 1750 and 1700 Ma because the regional metamorphism that produced the quartzite has been dated to

~1700 to 1600 Ma (Karlstrom and Bowring, 1991). Skotnicki et al. (1997) originally interpreted the mica-schist to be rhyolite, although he later changed this interpretation to be more intimately related to the surrounding quartzite (Skotnicki, 2014). Foliation, folds, crenulation cleavage, and kink-banding indicate two to three distinct deformation events in ductile, semi-ductile and semi-brittle environments at moderate depths and moderate to high temperatures. The sense of shear in this sample is less certain than in other samples. A minor overprinting of retrograde mica-chlorite mineralization may be present, which may impart the light green color. The relatively minor amount of antimony found in this sample and the surrounding quartz veins may indicate circulation of fluids were pervasive at shallow to moderate depths in permeable zones such as the shear zone and surrounding fractures.

2.2.3 Sample F4: Banded Mylonite

Sample F4 Observations

This sample was collected near the center of the shear zone across from the main milky quartz deposit (Figure 13 and Figure 19). This sample contains approximately 60 to 70% very fine-grained recrystallized quartz, 10 to 20% muscovite mica, 10 to 15% recrystallized feldspars (?) and 5% opaque minerals. Many minerals believed to be feldspar appear to be replaced with fine-grained mica minerals by a processes referred to as “sericitization”. Analysis in thin section revealed a strong mylonitic texture, possibly an ultra-mylonite texture (Figure 20). Many teardrop-shaped porphyritic augens made of an unknown opaque mineral appear to have been the most competent mineral grain. Mica and quartz are “wrapped” around opaque grains, and in some cases new quartz growth was observed on the trailing edges of opaque grains during shearing, referred to as pressure shadows. Pressure shadows reveal the sense of motion, and in this sample, strongly indicated a left-lateral or sinistral sense of shear. Post-shearing microscopic-scale brittle deformation was observed in thin section. Chlorite was observed as inclusions in quartz and fillings in veins and voids. Very thin, equigranular and polycrystalline quartz veins were also observed cutting across all other older textures. XRF analysis detected relatively small amounts of strontium, rubidium and copper, and relatively more abundant iron, manganese, antimony and tin (Table 2).



Figure 19. Sample F4 with diagnostic banded colors and very fine-grained texture.

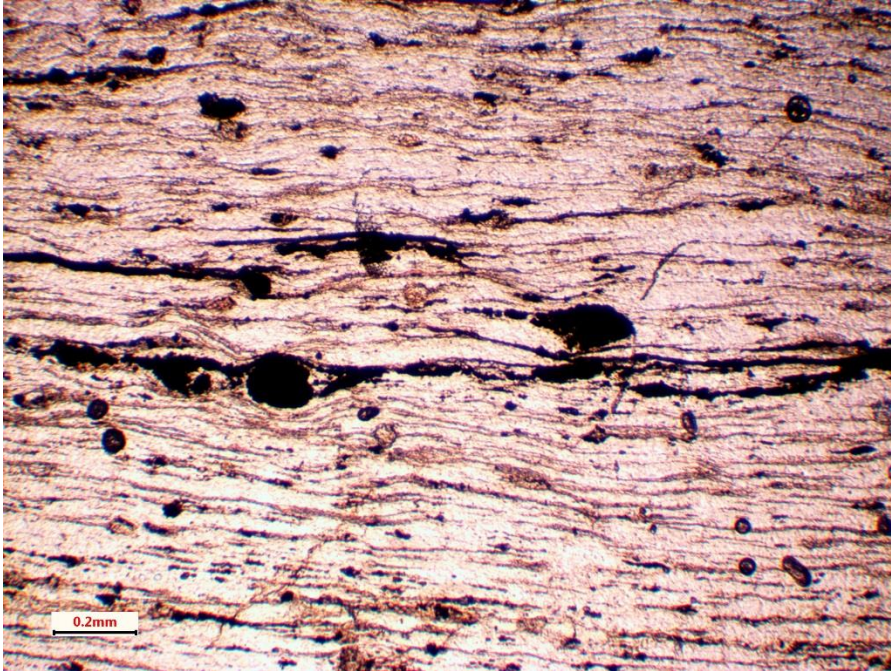


Figure 20. Sample F4 photomicrograph of finely-laminated mica-quartz mylonite. Scale in bottom left is 0.2 mm wide.

Sample F4 Interpretations

Based on the mineral composition and percentage, and the strong contrast in texture and color to adjacent mica-schist and quartzite, the protolith of this mylonite likely was granite, although the possibility of an immature quartzite cannot be ruled out. The original rock is strongly metamorphosed and pervasively sheared with a well-developed mylonite texture. The degree of shearing in contrast to the apparently less-sheared mica-schist may be a function of the parent rock and mineral type, i.e. a less-competent rock type in the shear zone. During the late stages of shearing, or following shearing of this rock, brittle or semi-brittle deformation occurred. If Sample F4 was originally granite, then shearing occurred after granite intruded (~1,425 Ma) and may be related to deformation associated with the Greenville Orogeny around 1,200 to 1,100 Ma (Skotnicki, personal communication). Peak metamorphic conditions suitable for formation of ductile and semi-brittle shearing of quartz-rich rocks may likely be between 10 to 20 km (6 to 12 mi) and 300 to 500 °C (550 to 900 °F) (Brace and Kohlstedt, 1980); however, conditions of mylonitization can depend on the presence of water, pore pressure and strain rate.

While at moderate to shallow depths and/or low-grade temperatures, sericite and chlorite mineralization overprinted previous minerals. The presence of tin, antimony, manganese and copper may indicate the presence of sulfide-bearing mineralization via groundwater circulation, although specific minerals, if present, could not be identified in thin section or hand sample. Due to the lack of well-developed retrograde mineralization, assigning an age to low-grade mineralization would be dubious. Brittle fractures and joints post-date deformation textures and are filled with euhedral quartz and chlorite, probably at much shallower depths.

2.2.4 Sample F5: Quartzite

Sample F5 Observations

Sample F5 was collected from exceptionally well-preserved quartzite immediately west and just outside the mapping area (See Figure 11). A few meters west of this location granite has an intrusive contact relationship with quartzite. Sample F5 was chosen due to the remarkably well preserved primary cross-bedding and lack of deformation. The quartzite contains 98% quartz, 1 to 2% muscovite mica, and approximately 1% opaque minerals. Zircon grains were also found (Figure 21). Muscovite mica grains are subparallel, probably related to original compaction of sandstone. Individual quartz grains have randomly oriented axes, further indicating lack of deformation. Grain and subgrain boundaries are highly serrated indicating a strong recrystalliation texture. Approximately 2% chlorite, probably an iron-rich variety, is pervasive throughout the sample as fine-grained to very fine-grained acicular blades growing across grain boundaries (Figure 22). Relatively abundant iron, and minor amounts of rubidium and arsenic were detected by XRF analysis (Table 2). The abundance of iron may represent iron-bearing oxides, mica and opaque minerals.

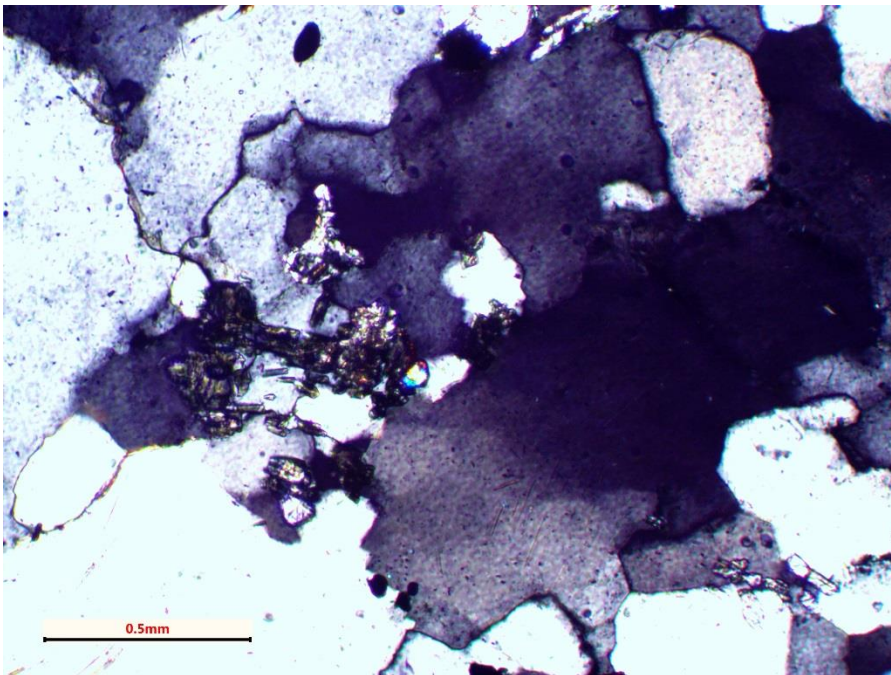


Figure 21. Sample F5 photomicrograph showing equigranular, non-foliated quartz with rounded zircon grain in center. Scale in lower left is 0.5 mm wide.

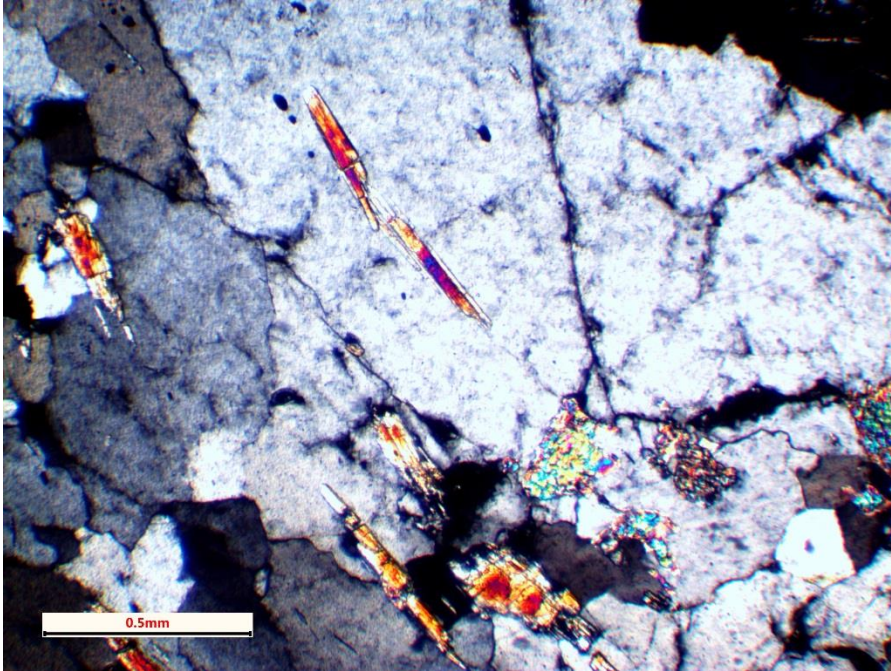


Figure 22. Sample F5 photomicrograph showing sheet-like chlorite cutting across quartz grain boundaries. Blocky muscovite mica seen in lower right with dense color hues. Scale in lower left is 0.5 mm wide.

Sample F5 Interpretations

This sample is a representative sample of clean, non-deformed fine to medium-grained quartzite. The protolith is interpreted to have been a sandstone deposited in a subaerial environment, possibly eolian. Cross-bedding indicates moderately tilted bedding with stratigraphic top direction to the northwest. The strong recrystallization textures suggest moderate depth and temperature: 4 to 6 kilobars (12 to 18 km or 7 to 11 miles depth), 350 to 450 °C (660 to 840 °F) (Couch, 1981), likely the original metamorphic fabric created during regional metamorphism around 1,650 to 1,600 Ma (Couch, 1981; Williams, 1991; Lund et al., 2015). Chlorite mineralization post-dates metamorphism and may represent low-grade retrograde metamorphism during uplift or cooling, or a consequence of elevated temperatures and contact metamorphism from nearby granite intruded circa 1,425 Ma, or a combination of both. Quartz veins or pegmatite veins were not observed emanating from the granite into quartzite.

2.2.1 Sample F6: Mica-Quartzite

Sample F6 Observations

Similar to Sample F5, Sample F6 was collected from non-deformed quartzite but east of the shear zone. Primary bedding was not observed in this area. This sample consists of 97 to 98% fine-grained anhedral quartz, 2 to 3% muscovite mica, and 1 to 2% opaque minerals. The protolith rock is sandstone. A thin quartz vein cutting across the quartzite and about 1 cm thick was also present in the sample thin section (Figure 23).

The quartz vein is very pure quartz with no other apparent minerals. The quartz vein is uniaxial with crystallographically subparallel subgrains resulting from high-temperature deformation. Foreign blocks of quartz and mica derived from the vein wall are surrounded by the quartz vein (also

referred to as xenocrysts). The boundary of the quartz vein with quartzite is apparently sharp in hand sample, but highly irregular in thin section (Figure 23).

Very thin deformation bands or gashes are present in the quartz vein (Figure 23 and Figure 24). An unknown brown mineral inclusion and possibly fluid inclusions are present in the cores of each band, which is associated with the white milky appearance in hand sample. Fluid inclusions may be present but were not observed at 50X power. Deformation bands do not penetrate the quartzite. Quartz subgrains in the parent rock appear finer grained along vein margins, suggesting quartz recrystallization of the parent rock occurred after the deformation of the quartz vein. Minor chlorite is present in the quartzite, but not apparent in the quartz vein. At least two brittle deformation events post-date the quartz vein and its deformation.

The XRF spectrometer targeted quartzite and vein portions of sample F6 separately. In quartzite, strontium, rubidium and iron were detected. The quartz vein had similar amounts of the elements detected in the quartzite host rock; however, it contained one-third less iron, and new elements copper, antimony, tin and cadmium (Table 2).

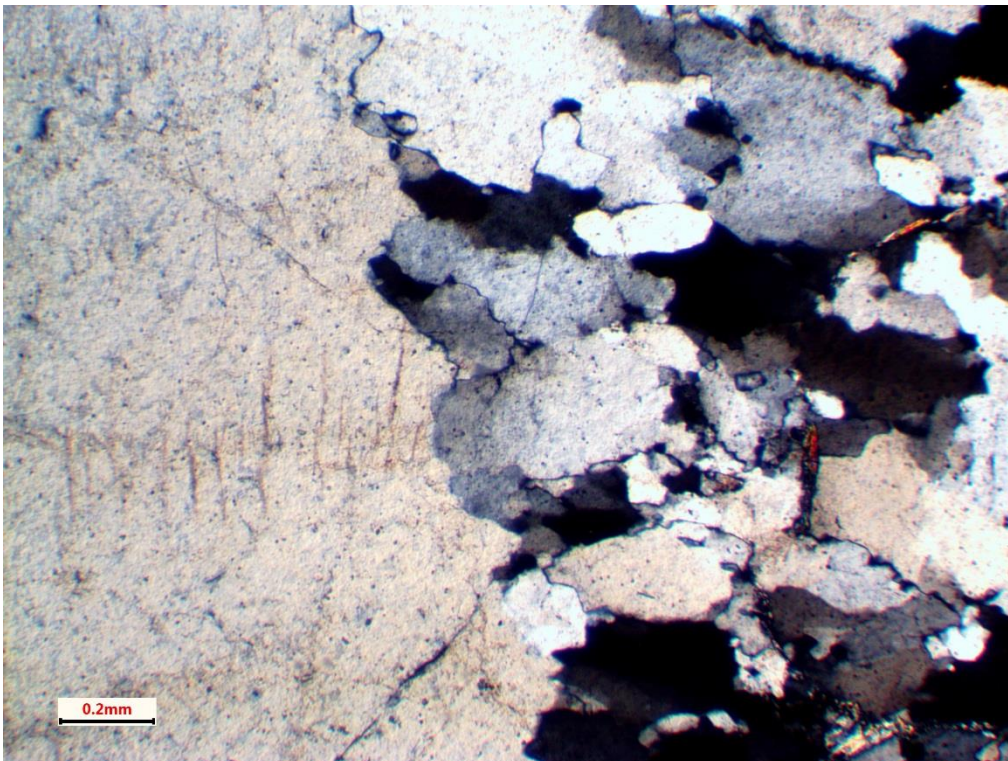


Figure 23. Sample F6 photomicrograph with quartz vein (left) in sharp contact with its host rock quartzite (right). Notice wispy brown lines (deformation bands) in vein, enlarged in Figure 24. Scale in bottom left is 0.2 mm wide.

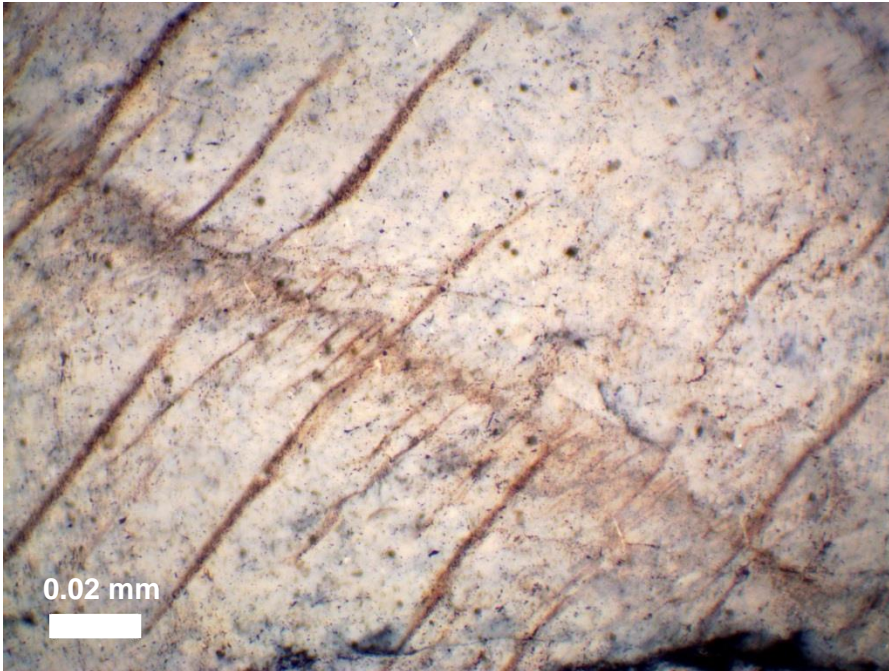


Figure 24. Sample F6 photomicrograph showing multiple generations of wispy *en echelon* deformation bands or gashes in the quartz vein seen at a smaller scale in Figure 23.

Sample F6 Interpretations

Sample F6 is a non-deformed micaceous quartzite with a sandstone protolith. Quartz is moderately to strongly recrystallized with minor secondary chlorite. The quartz vein was formed during the late stages or following regional metamorphism of this rock, and occurred under semi-brittle to brittle conditions. Multiple generations of wispy deformation bands and gashes appear to have formed during or immediately following vein formation. Unknown brown mineral (and fluid?) inclusions are well-preserved in these microscopic gashes, yet appear white under a hand lens and in the outcrop. At least two sets of brittle fractures post-date all of these textures. The presence of antimony, copper, tin and cadmium found in the quartz vein but not quartzite may indicate a concentrated hydrothermal fluid from an unknown source circulated prior to crystallization of quartz. These elements are likely associated with sulfide minerals (SbS, CuS, etc.) emplaced at moderate to shallow depths.

2.2.1 Sample F7: Mica-Quartz Mylonite

Sample F7 Observations

Sample F7 was collected from the southwestern-most extent of the study area, primarily to determine the original rock type prior to shearing, and to help constrain age relationships in the study area (Figure 13). This sample is technically a foliated mica-quartz schist or mylonite. Foliation ranges from moderate to strong. This sample consists of approximately 45% quartz, 35% muscovite and possibly biotite mica, 15% opaque minerals, 10% chlorite and 5% iron-oxide minerals, with an overall fine to medium-grained texture. Opaque minerals appear to be the most competent mineral and are preserved as augens surrounded by muscovite mica; however, quartz, feldspar, possibly mica and clumps of quartz crystals were also seen to form augens. The matrix is predominantly muscovite mica. Opaque minerals also post-date foliation and grew into and across other minerals (Figure 25).

One quartz vein was observed cutting across foliation, and was significantly fractured and embayed by other minerals. Sense of shear indicators were too difficult to discern. The quartz vein is polycrystalline, which may suggest growth into an open cavity filled with fluid under changing conditions. The quartz vein has undulose extinction suggesting mild strain due to stress. A very fine-grained chloritic (?) overprinting is present throughout the thin section. XRF analysis detected relatively low amounts of strontium, rubidium, lead and zinc, and a relatively high concentration of iron (50,300 +/- 1,000 ppm). The iron content may signify that sample F7 represents a different protolith than the mica-schist that dominates the shear zone.

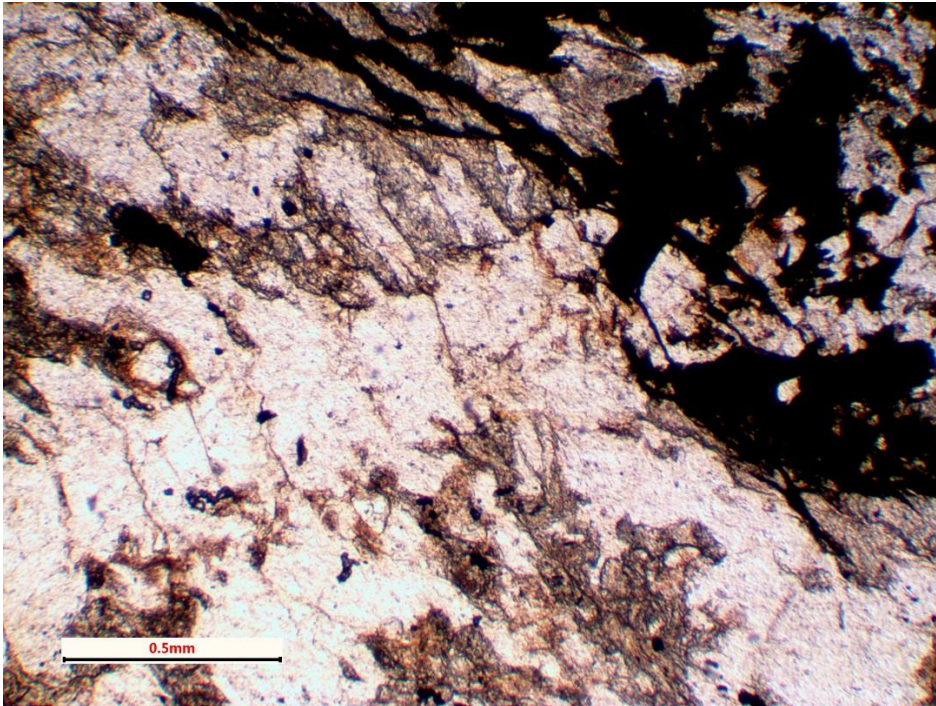


Figure 25. Sample F7 photomicrograph in plain polarized light. A thin quartz vein resembling vertebrae cuts across foliated rock from lower left to upper right. Foliated rock runs from upper left to lower right throughout the view, and has black opaque-rich bands in upper right and mica-rich bands in lower left. Clear areas are quartz and feldspar. Scale in bottom left is 0.5 mm wide.

Sample F7 Interpretations

Based on composition, color and compositional banding, proximity to granite bedrock, and iron content, the protolith of sample F7 is believed to have been granite. This sample is also similar in appearance to Sample F4, interpreted to be a granite protolith. This rock was observed inside the main shear zone, along its margin with non-deformed rock, and exhibits less deformation than the main shear zone and sample F4. Quartz veins formed after shearing. Chlorite, opaque and oxide mineralization were the last minerals to crystallize. The presence of lead and zinc may represent sulfide mineralization at shallow to moderate depths, although the timing of these minerals are not known.

2.3 Summary and Conclusions

Geologic mapping, detailed observations and thin-section analysis reveal important relationships between milky quartz, its host rock(s), relative age, and subsequent deformation and alteration. The following sequence of geologic events is a synthesis of geologic mapping combined with thin-section analysis:

1. 1,750 to 1,650 Ma: Deposition of sandstone followed by rapid burial, compaction and cementation. Deposition may overlap temporally with deformation associated with metamorphism related to the Mazatzal Orogeny (Lund et al., 2015).
2. 1,700 to 1,600 Ma: Metamorphism of sandstone into quartzite. Peak metamorphic conditions are not well constrained, but believed to have occurred around 1,650 to 1,620 Ma (Lund et al., 2015) and be generally low-grade between 250 and 350 °C (~500 and 650 °F) (Karlstrom and Bowring, 1991; Gillentine and others, 1991). Groundwater trapped following deposition of sandstone was probably retained while the rock was being rapidly buried prior to metamorphism. Towards the end-stage of burial and metamorphism, hydrothermal conditions may have been prime for the formation of relatively non-deformed quartz veins along bedding planes. Veins would have likely been discontinuous and tabular and/or oblate in shape.

Note that the range of previously proposed dates are quite broad for deposition of sandstone (1,750 to 1,650 Ma) and for metamorphism (1,700 to 1,600 Ma), depending on location in the Proterozoic belts. For the McDowells there is some evidence (Skotnicki 2015, personal communication) that the dates for deposition, and likely metamorphism, are younger (closer to the more recent end of the ranges) than previously assumed (Doe et al., 2011).

3. 1,425 Ma: Intrusion of quartz-bearing granite at moderate depths, producing low-grade chloritic alteration in granite and non-deformed quartzite. Following or synchronous with chloritization, hydrothermal conditions appear to have been favorable for the continued formation of quartz veins in granite and quartzite at moderate depths and temperatures. Quartz veins underwent dynamic recrystallization and formed mineral and fluid inclusions along micro-fractures in quartz during mild to moderate conditions of dynamic stress.
4. 1,400 or 1,100 Ma: Quartzite, milky quartz and non-deformed granite rocks become deformed along a narrow shear zone, with a left-lateral sense of shear. Shearing may be associated with compression-related magmatism related to younger 1,400 Ma plutons in the region (Nyman et al., 1994), or tectonism related to the Grenville Orogeny around 1,100 Ma (Skotnicki, 2015, personal communication). Shearing is thought to have occurred at moderate depths, moderate to high temperatures, under ductile to semi-brittle conditions. Rocks are strongly foliated and locally folded and mylonitized. Granite protoliths exhibit a much higher degree of shear-foliation and shear-banding. Conversely, milky quartz and quartzite exhibit the least degree of foliation. Additional mineral and fluid inclusions are formed in milky quartz and superimposed on previous inclusions. Quartz minerals in rocks continue to recrystallize during shearing.

5. 1,400 or 1,100 Ma: Foliated rocks are subsequently deformed to produce a light crenulation cleavage, restricted (?) to foliated rocks in the shear zone at temperatures of approximately 250 to 400 °C. This may represent uplift to more brittle environments, waning of orogenesis in the region during 1,400 Ma magmatism, 1,100 Ma Grenville Orogeny, or a combination. Shortly following shearing quartz undergoes light to moderate recrystallization at temperatures of approximately 250 to 350 °C. The presence of tin and antimony in foliated rocks and quartz veins in and around the shear zone may indicate circulation of sulfide-bearing fluids in permeable foliated rock and open fractures, although the timing of this emplacement in relation to shearing is not well constrained.
6. 1,400 or 1,100 Ma: A minor amount of retrograde chloritization appears to have followed shearing and subsequent recrystallization, indicating rocks are still at moderate depths and temperatures. Chloritization could be associated with retrograde metamorphic conditions after the Carefree granite intruded around 1,400 Ma. Alternatively, chloritization may be related to widespread and pervasive low-grade metamorphism between 100 and 280 °C associated with voluminous intrusions of diorite circa 1,100 Ma known to have occurred in the region (Gillentine and others, 1991; Bright et al., 2015).
7. 700 to 10 Ma (?): Rocks are uplifted to more shallow and/or brittle conditions, which form minor brittle textures cross-cutting older textures. More than one episode of brittle deformation such as fractures and joints are present but not as abundant as older deformation textures. Oxide mineralization has occurred along permeable micro-fractures and along micaceous minerals exposed along fractures and surfaces. Several geologic events span this time range, which include uplift, exposure, compression and extension.

The source of fluids which allowed for the formation of milky quartz remains unknown. Fluid-inclusion analysis to determine the salinity, temperature, and depth of emplacement was unfeasible due to the degree, age and complexity of quartz formation. Depth and temperature of quartz formation remain unclear; however, regional and local studies of similar age rocks place the formation of quartz in a range between 4 and 6 kilobars [12 to 18 km depth], and 350 to 450 °C [660 to 840 °F] (Couch, 1981; Karlstrom, 1991). Additional research to refine the geobarometry and geothermometry is needed.

There is no evidence in the study area of quartz or pegmatite veins extending from the nearby granite bedrock into quartzite. Therefore it seems unlikely that magmatic fluids associated with the granitic magma were the primary source for the main milky quartz deposits observed at the site. Instead, we propose that meteoric groundwater still trapped in local sandstone prior to the Mazatzal Orogeny around 1,700 to 1,600 Ma was the likely source fluids for the original formation of milky quartz along bedding planes.

3.0 Paraiso Site

3.1 Geologic mapping

The Paraiso site consists of isolated hills and knobs of granite, pegmatite and milky quartz located at the base of McDowell Mountains along the uppermost piedmont (See location map in Figure 26). Reconnaissance geologic mapping revealed numerous rock types and features associated with the massive milky quartz deposits (Figure 26). A more detailed geologic core map is shown in Figure 27.

Three main geologic units characterize bedrock at Paraiso: 1. A coarse-grained granite (Ygc), 2. A megacrystic pegmatite of feldspar, tourmaline and quartz (Yp), and 3. Massive milky quartz (Ymq). Other notable rock types include fine-grained granite, an orbicular granite, epidote veins, and xenoliths of older rocks. A thin veneer of grus and colluvium represents the most extensive mappable unit. Each geologic unit is described in general in Figure 26 and in more detail below.

3.1.1 Carefree Granite (Yg)

The coarse-grained granite is widespread from the northeastern end of the McDowell Mountains at Toms Thumb, across the piedmont to the north and northwest towards Cave Creek. The granite in Paraiso is thought to be equivalent to the Carefree or Pinnacle Peak Granite, emplaced $1,422.5 \pm 2.2$ Ma (Isachsen and others, 1999; Skotnicki, 2015 personal communication). The granite has a porphyritic texture, with coarse-grained crystals of pink potassium-feldspar 3 to 4 cm long in a matrix of finer-grained (although still coarse-grained) gray quartz, black biotite, and plagioclase, all less than 1.5 cm across (Skotnicki, 2014) (Figure 28). Finer-grained granite with a similar mode as the coarse-grained granite is also present at Paraiso, and commonly found near the margins of milky quartz (Figure 30). Granite weathers into crystal-size clasts, referred to as grus, which are easily transported into small gullies. In contrast, milky quartz weathers much more slowly. The resulting landform associated with milky quartz in granite is a cone-shaped hill with knobs of quartz at the top.

3.1.2 Milky Quartz (Ymq)

Massive milky quartz veins are the most visually prominent features at Paraiso. They are exposed in erosional relief in contrast to easily weathered and eroded granite (Figure 29). The milky quartz was originally mapped and described as milky quartz veins surrounded by granite (Skotnicki, 1996). Milky quartz within granite is exposed in other areas along the piedmont; however, very little was known about the source, emplacement history and age of quartz. Through geologic mapping, it became evident that the milky quartz is encircled in a zone of coarse crystals referred to as a pegmatite. Thus, the milky quartz at Paraiso is actually the core of the pegmatite, where the outer pegmatite zones (unit Yp) are described in the next section.

Geometries of milky quartz and pegmatite appear to have a cylindrical, cone or elliptical shape, rather than a lenticular or tabular shape commonly seen in metamorphic rocks throughout the Preserve. The size of milky quartz and pegmatite crystals are quite large. This type of milky quartz is often referred to as “bull quartz”. The size of milky quartz crystals is unknown due to fracturing and obscurity, but based on observation, individual quartz crystals are suspected to be at least as large as surrounding feldspar crystals, on the order of several feet or meters, and weighing several thousand kilograms (several tons). Where visible, feldspar crystals are a meter (~3 ft) or more with crystal ends often obscured by sediment. These mega-crystals have euhedral crystal faces, although some areas

the faces may be subhedral or anhedral. The milky quartz has abundant fractures yet it is highly resistant to chemical weathering. Algae often grow at the surface along fractures and on the underside of quartz clasts. Eolian silt and clay percolate through the fractures and coat quartz with a brick and iron color. The milky white color is produced by light that reflected off trillions of microscopic mineral and fluid inclusions in the quartz found along microscopic hairline fractures (Figure 31). Variations in color range from transparent, milky, gray, to rose. Cobble and boulder size quartz blocks form a colluvial lag on slopes as finer-grained grus and quartz clasts are transported down slope (unit Qcq).

3.1.3 Pegmatite (Yp)

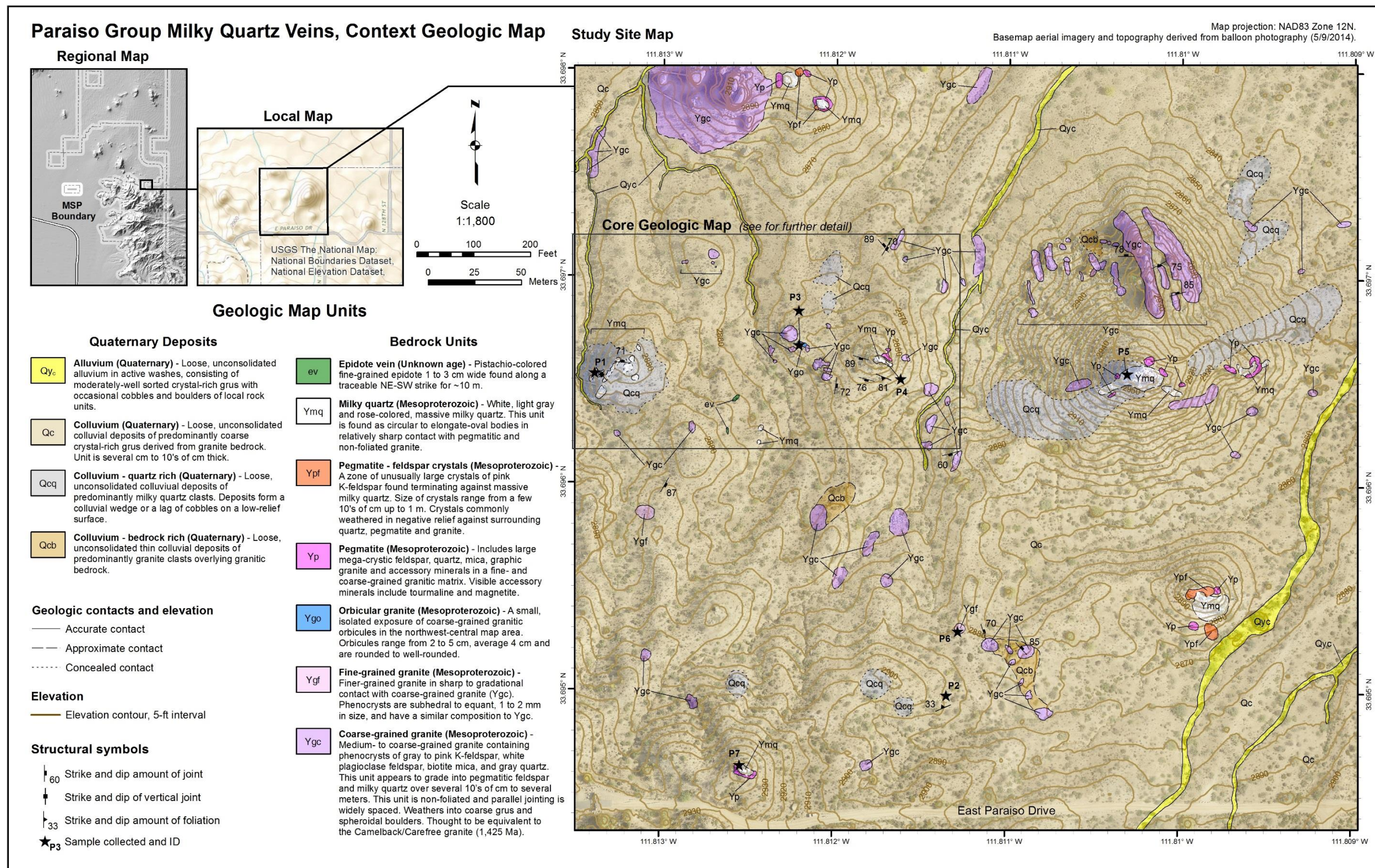
At Paraiso, the milky quartz is uniquely associated with megacrystic feldspar and graphic granite surrounding a core of milky quartz. Due to the composition and size of the constituent crystals, this configuration is referred to as a granitic pegmatite. A granite pegmatite is an intrusive igneous rock with coarse to gigantic-sized crystals of feldspar. This composition was discovered by the mapping team and is shown in Figure 26 and Figure 27. Large individual euhedral crystals of feldspar and/or graphic granite, up to one meter long, are observed in sharp contact with milky quartz (Figure 32). Black tourmaline, also known as schorl tourmaline, an aluminum-boron silicate mineral, is also found radiating inward along the wall margins of milky quartz core (Figure 33).

For a given pegmatite, assemblages or lithologies of mineral species form concentric zones surrounding a core of milky quartz. Such zones are recognized in other pegmatites in the Arizona Pegmatite Belt, termed as having a boundary zone, wall zone, intermediate zone and core (Jahns, 1952 and 1953). Northeast of Bartlett Dam in the Maverick Mountain area are similar pegmatite/quartz concentric cores surrounded by granite. These core zones are interpreted as related to late-stage crystallization of the granite (Skotnicki and Leighty, 1998). Zoning is apparent in the Paraiso pegmatites, although mapping them on a mineral-species level was not a part of this study.

Geochemically altered granite can also form pegmatites at relatively shallow depths (0 to 5 km deep), to produce a rock type called greisen. Greisens may contain tin, gold, silver and other precious metals. Based on the apparent lack of these metals, and the generally well-preserved granite around the milky quartz and pegmatite cores, a greisen environment can be ruled out.

One of the unexpected discoveries at Paraiso was a relatively rare rock called orbicular granite. Orbicular granite was found as a series of small outcrops approximately 5 m long, 1 m wide and 1 m high (Figure 34). This type of granite is more closely associated with the coarse and fine-grained grained granite than the pegmatite. The orbicular granite was sampled (Sample P3) and is discussed further in the next section. A single conspicuous orbicule was found ~60 m (200 ft) southeast of Sample P3 (Figure 35).

The shape and relationships between pegmatites and granite are unknown. Geologic mapping revealed that the pegmatite bodies are isolated circular to irregularly oblate bodies. At depth bodies may merge or pinch out. Their geometry suggests that the bodies are more like steeply dipping pods or cavities (also referred to as miaroles or miarolitic cavities) rather than veins, dikes or large isolated bodies. Given the extent of granite between Cave Creek and the McDowell Mountains, and assuming the granite is similar in age and occurrence over its extent, one might expect a pod-like geometry to be exposed as isolated features by differential weathering and erosion.



C:\Data\Current Projects\McDowells\projects\Paraiso Context.mxd

Last updated: 5/2/2015

Figure 26. Paraiso context geologic map and legend.



Figure 28. Coarse-grained granite porphyry with large phenocrysts of potassium feldspar. Six-inch ruler for scale.



Figure 29. Milky quartz vein being described by MSC volunteers.



Figure 30. Fine-grained granite with phenocrysts of anhedral magnetite up to 1.5 cm across.

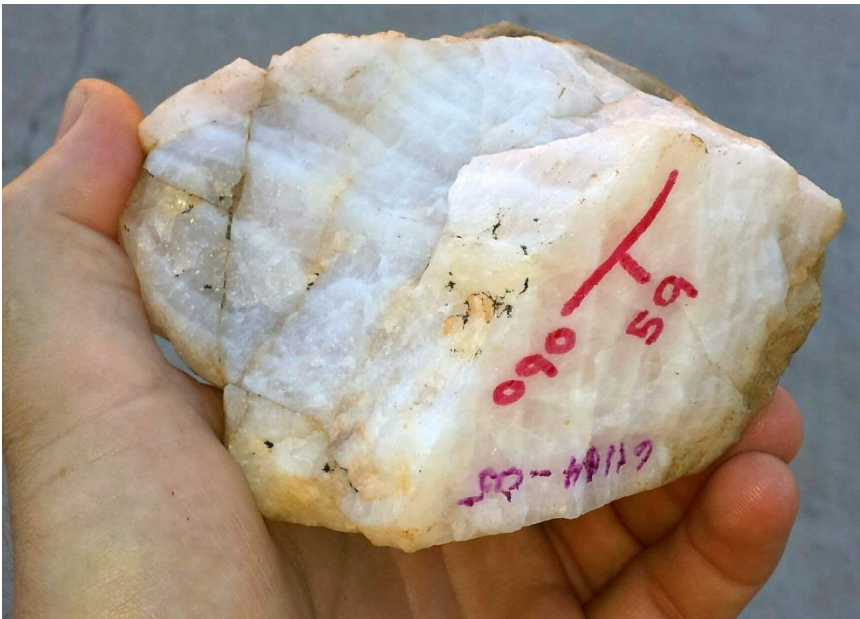


Figure 31. Milky quartz sample P5 before being cut or thin section analysis. Notice the slight rose color, white banding, and black specs of algae.



Figure 32. Cast and remnant of an individual feldspar crystal (reddish color) seen at the boundary of a milky quartz "core" (gray to white). Six-inch ruler for scale.



Qua

Figure 33. Tourmaline crystals commonly found at the boundary between milky quartz and mega-crystic feldspar. These are usually acicular and radiating into milky quartz.



Figure 34. An isolated outcrop of orbicular granite. Outcrop is approximately 3 feet high by 3 feet wide.



Figure 35. Conspicuous granite orbicule encased in relatively fine-grained granite in contact with coarse-grained granite typical of the Carefree granite. This is located ~60 meters southeast of Sample P4. Map board and pen for scale.

3.2 Rock Sample Analysis and Interpretations

Following geologic mapping at Paraiso a total of seven samples were collected for slab, thin-section and fluid-inclusion analyses. All samples are plotted in the context geologic map (See Figure 26) and listed in Appendix B. Three samples of massive milky quartz were submitted to Jim Reynolds of Fluid Inc. to evaluate the existence and condition of fluid inclusions preserved in quartz. Two samples had slabs made for mesoscopic study. The remaining samples were cut for thin section. Below are descriptions and interpretations from each sample collected at Paraiso. X-Ray Fluorescence (XRF) analyzer results for Paraiso samples are listed in Table 3.

Table 3. Results of the XRF spectroscopy analyzer used on Paraiso samples.

Sample and Elements. Concentrations in parts per million (ppm)	Paraiso											
	P1: graphic granite	P2: mylonite	P3: orbicular granite			P4: milky quartz	P4: tourmaline + quartz	P5: milky quartz	P6: fine- grained granite	P7: milky quartz	161-3: rose quartz	061114-04: unknown crystal
			CORE	RIM	MATRIX							
Strontium (Sr)	39 ± 7	220 ± 13	505 ± 15	227 ± 18	537 ± 21	--	15 ± 5	--	160 ± 13	--	--	17.2 ± 7.4
Rubidium (Rb)	485 ± 21	--	44 ± 5	228 ± 22	90 ± 10	--	--	--	27 ± 7	--	--	9.4 ± 6.1
Lead (Pb)	52 ± 15	--	28 ± 10	--	30 ± 13	--	--	--	29 ± 13	--	--	26 ± 16
Zinc (Zn)	--	70 ± 23	53 ± 16	305 ± 66	131 ± 30	--	72 ± 21	--	57 ± 42	--	--	--
Copper (Cu)	55 ± 28	--	43 ± 19	97 ± 51	111 ± 35	--	62 ± 24	--	--	--	--	85 ± 42
Iron (Fe)	182 ± 80	15,600 ± 500	18,000 ± 4,000	350,100 ± 2,900	50,300 ± 900	--	58,500 ± 800	--	14,500 ± 500	--	--	92,300 ± 1,500
Manganese (Mn)	151 ± 78	1,407 ± 255	445 ± 89	5,374 ± 531	1,019 ± 181	--	852 ± 142	84 ± 56	845 ± 171	--	--	435 ± 200
Chromium (Cr)	--	--	--	--	--	--	--	--	--	--	--	--
Antimony (Sb)	293 ± 95	--	--	--	--	--	338 ± 98	183 ± 84	--	144 ± 80	224 ± 80	630 ± 134
Tin (Sn)	342 ± 97	--	--	--	--	--	274 ± 100	132 ± 85	--	174 ± 83	200 ± 81	425 ± 136
Cadmium (Cd)	128 ± 61	--	--	--	--	--	126 ± 63	--	--	--	103 ± 51	118 ± 58
Uranium (U)	37 ± 23	--	--	45 ± 28	--	--	--	--	--	--	--	26.9 ± 15.8
Nickel (Ni)	--	--	--	248 ± 125	--	--	121 ± 46	--	--	--	--	198 ± 87
Mercury (Hg)	--	--	--	--	--	--	--	--	17 ± 9	9.3 ± 5.7	--	--
Silver (Ag)	--	--	--	--	--	--	73 ± 43	--	--	--	--	188 ± 58
Arsenic (As)	--	--	--	--	--	--	--	--	--	--	--	42 ± 16
Gold (Au), Cobalt (Co), Platinum (Pt), Chromium (Cr)	--	--	--	--	--	--	--	--	--	--	--	--

-- = may be present in low concentrations, but non-detected in XRF

3.2.1 Sample P1: Graphic Granite

Sample P1 Observations

Sample P1 was collected from the margin of milky quartz in an exposure too small to be shown on the geologic map (Figure 27). The graphic granite is light white to light pink, coarse-crystalline potassium feldspar with graphic interstitial quartz resembling flattened boomerangs or wedge-shaped (cuneiform) writing (Figure 36). Feldspar is considered the primary host mineral and exhibits a uniform crystal cleavage (i.e. it is one crystal) in hand sample and in outcrop over tens of cm where exposed. Nearly equal portions of microcline and albite forms of feldspar are present and appear to be intergrown with each other, which accounts for the mix of white and pink coloration. In thin section, intergrown quartz crystals form thin dome- or cup-like shapes, which are crystallographically uniaxial individually and collectively throughout the thin section in cross-polarized light (Figure 37).

Quartz exhibits one primary direction of undulose extinction, although a minor second one is visible at nearly 90 degrees. Micro-autoliths of disoriented feldspar appear to float inside quartz cuneiforms. Primary quartz crystals have been recrystallized along the margin of cuneiforms, and in some cases nearly completely recrystallized. Mica is present as a trace mineral. XRF analysis of Sample P1 yielded several metals with the highest concentration of rubidium (Table 3). In comparison with milky quartz, orbicular granite and tourmaline-quartz, Sample P1 is relatively low in strontium, high in rubidium, high in lead, low in iron and manganese, and high in tin.



Figure 36. Sample P1 thin section blank (left) and hand sample (right) of graphic granite. Minerals include albite feldspar (light gray), microcline feldspar (pink) and quartz (translucent medium gray) as part of one larger crystal entirely visible. The black line represents the location of the thin section blank. The scale is in centimeters.

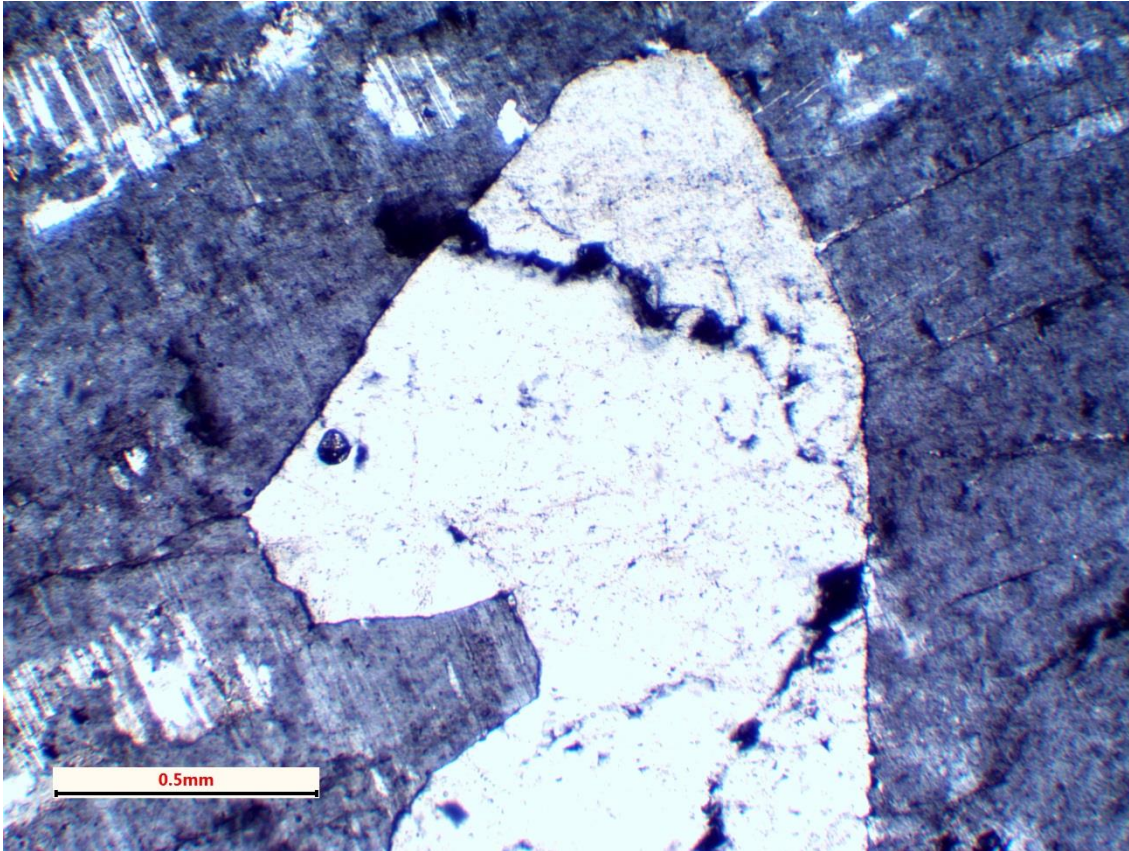


Figure 37. Sample P1 photomicrograph in cross-polarized light showing intergrown microcline and albite feldspar (dark regions with showings of synthetic twinning [microcline feldspar]). In the center is the edge of a single quartz cuneiform crystal intergrown within feldspar. Scale in lower left is 0.5 mm wide.

Sample P1 Interpretations

The graphic granite is interpreted to have crystallized from a fractionated melt during the late stages of granite formation and early phase of pegmatite growth. Where visible, the graphic granite is between the granite host (Yg) and milky quartz (Ymq) and may represent a wall margin of the pegmatite. The formation of graphic granite is interpreted to represent the simultaneous growth of two phases of supersaturated melt at constant rates under conditions which favor feldspar growth combined with interstitial quartz (Wahlstrom, 1939; Fenn, 1986). In theory, graphic granite could have crystallized at temperatures below 500 °C (Simmons and Weber, 2008).

The relative equal distributions of albite and microcline feldspar appear to be intergrown, although albite may have replaced microcline. Partial recrystallization of quartz cuneiforms exists, although its timing is not certain. Recrystallization of quartz and feldspar may have occurred at a similar time, although this could not be determined. The two distinct undulating extinctions at near 90 degrees suggest strain in two directions, possibly associated with the crystallization process.

3.2.1 Sample P2: Gneiss or Mylonite

Sample P2 Observations

Sample P2 was collected from a strongly layered gneissic or mylonitic rock in the southeastern portion of the context area (Figure 26). A strike and dip of foliation was measured, although it is not clear if the rock is in-situ or has been rotated due to slope creep (Figure 38). The rock was not in contact with other rock types, nor was it large enough to be mapped. It was sampled for slabbing and visual inspection only to determine the protolith and context to the study area. Sample P2 is a light olive-gray brown, fine- to medium-grained layered gneiss or mylonite. It has thin to laminated bands of alternating olive-gray, white to light gray and dark gray colors. Dark gray layers have sub-millimeter opaque subhedral laths in a fine-grained matrix. Lighter bands have light green specks in a fine-grained matrix. The light green specks are interpreted to be products of chloritic alteration. The sense of shear and protolith could not be determined with a hand lens.



Figure 38. Sample P2 collected from this outcrop of gneiss or mylonite. Layering is tilted towards the northwest. Height of outcrop approximately 1 meter.

Sample P2 Interpretations

The low angle and lack of continuous exposure into other rocks along the same strike seem to suggest this is a xenolith of older country rock rather than an in-situ shear zone cutting granite. However, northeast-striking, steeply-dipping mylonite zones observed cross-cutting the same granite have been mapped in the vicinity of this site (Skotnicki, 1996). The degree of chloritization was not definitive enough to compare with chlorite present in other rocks. Thus the origin, relationship to other units, and relative age of this exposure is obscure.

3.2.1 Sample P3: Orbicular Granite

Sample P3 Observations

During geologic mapping in the core mapping area an uncommon type of granite called orbicular granite was discovered by the mapping team (Figure 27 and Figure 34). Exposure of this granite is isolated to only a few square meters and was found in contact with fine-grained granite (Figure 39). Orbicular granite is defined as having spheroidal shaped structures (orbicules) surrounded by a matrix with one or more concentric shells of contrasting mineral composition and texture, and radiating or tangentially oriented minerals (Levenson, 1966).



Figure 39. Fine-grained granite at locality P3, with embedded orbicules. Outcrop considered to be in-situ and is estimated to approximately 0.6 m (2 feet) wide.

At Paraiso, the orbicules consist of a core, commonly two to three concentric shells, and a matrix. Orbicules are spherical and oblate, and range in size from 1 to 7 cm in length, averaging 4 to 5 cm long. The rock has a noticeably high specific gravity when hefted, which may be related to the magnetite content. Cores commonly consist of a single crystal of potassium feldspar (similar to the feldspar seen in coarse-grained granite), although cores of fine- and coarse-grained granite are also

present. Sample P3 was collected from this outcrop for thin-sections and slabs. A better view of the orbicules is seen in one of the slabs made (Figure 40).



Figure 40. Sample P3 of orbicular granite as a cut slab. Scale in centimeters. Cores consists of coarse-crystalline granite (far left center) or more commonly single sub- to anhedral potassium feldspar crystals (remaining orbs). Rims are defined by concentric dark-colored minerals biotite mica, hornblende and magnetite. The matrix consists of medium- to coarse-grained granite.

Two thin sections were made to observe the core, shell and matrix, Samples 3a and 3b.

Core:

As mentioned above, cores in Sample P3 consist predominantly of single potassium feldspar phenocrysts, although fine- and medium-grained granite can also make up a core (Figure 41). On the margins of single feldspar cores, but still within optically continuous feldspar, are inclusions of biotite and magnetite. The inclusions may have resulted from crystallization of the magma after feldspar crystallized, yet while the shell was forming (Figure 40). A moderate to abundant amount of fracturing of phenocrysts in the core is present, and sericitization is common along fractures. In orbicules with an orthoclase feldspar core, XRF analysis of the core had elements more similar to the fine-grained granite than any other lithology type tested (Table 3).

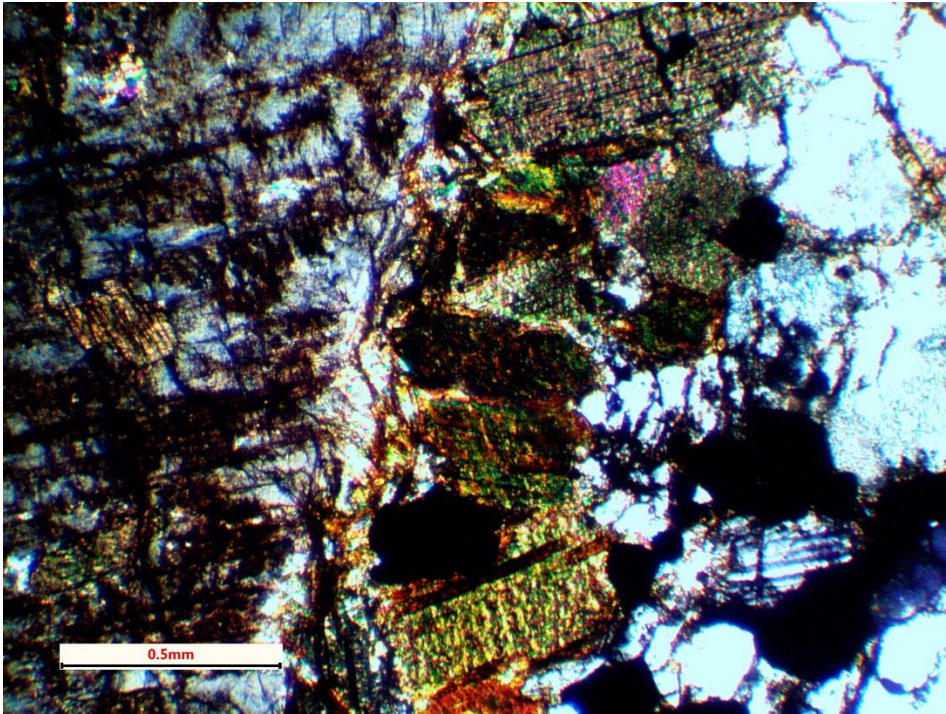


Figure 41. Sample 3b photomicrograph of orbicule orthoclase feldspar core (left), perpendicular biotite rim or shell (center) and granite matrix (right).

Rim or Shell:

Most orbicules are rimmed with one concentric shell, consisting of predominantly euhedral biotite (60%) and magnetite (40%). Biotite is in sharp contact and in most cases subparallel to the core, but can be perpendicular (Figure 41), oblique or combinations of all three. Biotite and magnetite decrease in size at the outer margin of the shell (Figure 42). Magnetite was identified in the field and hand sample based on its physical characteristics and magnetism, and by crystal shape in thin section. Thickness of the rim ranges from 2 to 7 mm thick. Subhedral to euhedral magnetite phenocrysts occur in the shell zone as a radiating line of phenocrysts between the core and matrix, where magnetite commonly cuts across single crystals of biotite, which may suggest the orbicules were solidified before the matrix completely solidified. XRF analysis of the rim is remarkably different than that of the core or matrix, consisting of a high iron, manganese, nickel, uranium, zinc and rubidium content relative to other samples (Table 3).

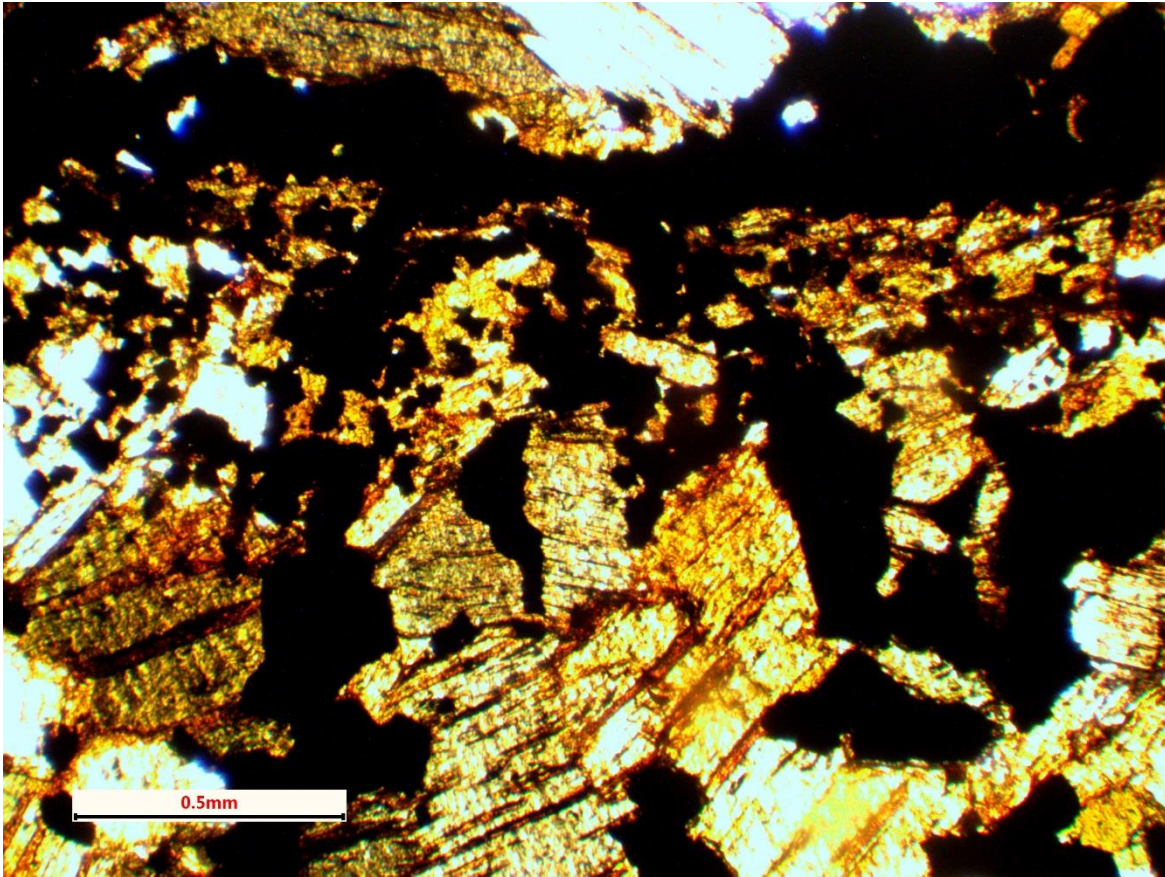


Figure 42. Sample 3b photomicrograph showing a portion of an orbicule shell several mm thick. Dark brown is predominantly biotite mica. Black areas are magnetite, with the horizontal band at top marking the outer boundary of the shell. Notice the nearly perpendicular line of magnetite phenocrysts, which, in many cases, cut across individual biotite phenocrysts. Also notice the decrease in grain size towards the outer shell. Scale in lower left is 0.5 mm wide.

Matrix:

The matrix between orbicules is generally medium- to coarse-grained granite with euhedral to subhedral interlocking crystals. Mineralogy in the matrix is distinctly different from the core, and consists of microcline feldspar, plagioclase feldspar, quartz, biotite, hornblende and magnetite, typical of the main granite observed at Paraiso. XRF analysis of the matrix, a coarse-grained granite, was more similar to the core than the shell although iron and manganese concentrations were about 2 to 3 times higher (Table 3).

Sample P3 Interpretations

Orbicular granite was only observed in contact with fine-grained granite and closely associated with coarse-grained granite nearby; however, the close proximity to numerous pegmatites in the study area seems to indicate that the orbicular granite is uniquely associated with the process and formation of pegmatites and milky quartz. Orbicular granite is interpreted to be associated with a water- and vapor-rich phase of melt from a granite batholith (Affholter and Lambert, 1982). In comparison to other orbicular granite worldwide, the Paraiso orbicules are apparently limited to a small extent and volume, have few concentric shells and are relatively small. This may suggest a restricted environment where

the process of forming orbicules was relatively quick and short-lived. Crystallization of the orbicules appears to have started from available seed material derived from the host granite, such as large orthoclase phenocrysts and pieces of fine- and coarse-grained granite, thus the orbicules are interpreted to have formed in a fluid-rich environment adjacent to solidified granite chambers or walls. The orbicules are interpreted to have been solid prior to solidification of the matrix. The iron to manganese ratio between the core, rim and matrix were very similar, ranging from 40:1 to 60:1, possibly indicating relatively minor fractionation between the formation of orbicules and the main phase of granite.

3.2.1 Sample P4, P5 and P7: Milky Quartz

Observations

Samples P4, P5 and P7 were collected from milky quartz “cores” (mapped in Figure 26 and Figure 27). All are remarkably similar in outcrop and thin section. Alternating bands and thin laminae of milky and transparent quartz were common and visible to the naked eye (Figure 31). Also visible are abundant irregular fractures and joints. In thin section the samples contained regions of uni-axial quartz or disseminated individual crystals of very fine-grained quartz (Figure 43).

Each sample was evaluated for fluid inclusions, including the preservation, size, texture and quality of fluid inclusions, by Jim Reynolds, who analyzed each of these samples in detail. Brian Gootee analyzed and photographed Sample P7. Each sample has wispy textures (from ubiquitous planes of inclusions crisscrossing back and forth), decrepitation textures (from exploding inclusions due to heating, or from burial or uplift paths), transposed planes (migration of inclusions off healed microfractures during recrystallization of quartz under strain), and double bubbles (due to the presence of CO₂ in the inclusions) (Reynolds, 2015). A relatively non-fractured portion of sample P7 allowed for a view of very fine-grained fluid inclusions at the petroscope’s highest magnification (Figure 44).

XRF analysis on milky quartz samples range from having no detectable heavy metal ore elements to concentrations of tin, antimony, mercury, nickel, uranium and other elements (Table 3). A sample of milky quartz with tourmaline was collected next to Sample P4. The sample with tourmaline intergrown with quartz had the most diverse concentrations of detectable elements, whereas sample P4 of pure milky quartz had none. In association with the milky quartz at Sample P5, a euhedral crystal of unknown type was collected from a cavity within milky quartz. The crystal was replaced with quartz, a quartz pseudomorph, which has the most diverse concentrations of elements, and may indicate the original crystal grew from a highly fractionated liquid.

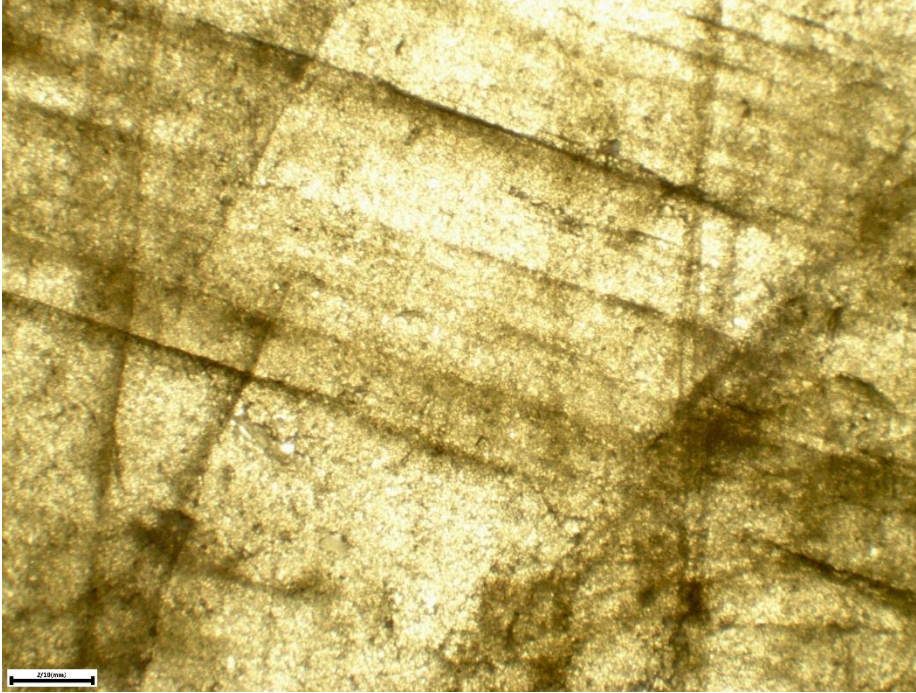


Figure 43. Sample P7 at 3X power showing very finely-laminated bands from upper left to lower right. Darker bands have more abundant mineral and possibly fluid inclusions. Joints and fractures cross-cut layers at nearly right angles and also are filled with microscopic inclusions. Scale in lower left is 0.2 mm wide.

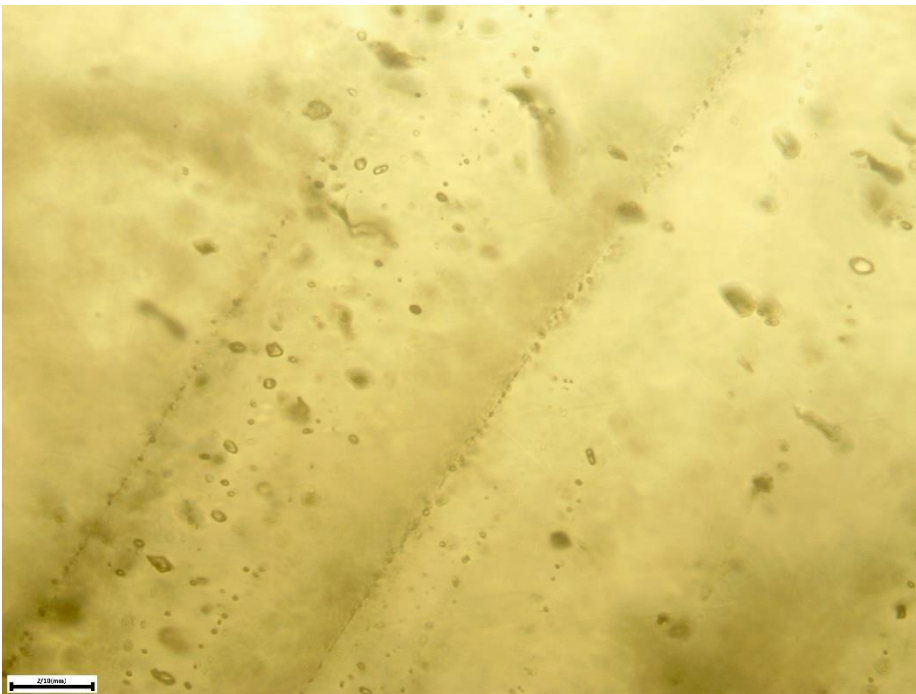


Figure 44. Sample P7 showing a relatively non-fractured portion at 25X power showing microscopic fluid and mineral inclusions, double-bubbles in between individual layers or bands. Thin section is 90 microns (0.09 mm) thick, which allows one to see additional inclusions as an out-of-focus texture at an oblique angle from the observer. Scale at lower left is 0.02 mm wide.

Interpretations

Based on wispy fractures, decrepitation, transposed planes and double-bubble textures observed in these samples, Jim Reynolds concluded the milky quartz underwent multiple generations of fracturing and annealing with new quartz and new fluid inclusions. Such textures are not common in shallower environments of vein formation, but are ubiquitous in deeper environments (Reynolds, personal communication, 2015). Formation of quartz and recrystallization of existing quartz would have occurred over many generations, potentially over a long time period. As a result, quantitative analysis of fluid inclusions would not have yielded specific or conclusive temperatures, salinities and depth of environment the quartz formed in. Further research may find small mineral or fluid inclusions in tourmaline, beryl or spodumene commonly found in pegmatites in the region (Jahns, 1953). Interpreting the results of XRF analyses are not clear. The variety may indicate milky quartz sampled at P4, P5 and P7 formed under similar conditions but different chemistry, perhaps at different times.

3.2.2 Sample P6: Fine-grained Granite

Sample P6 Observations

Sample P6 was collected from the fine-grained granite unit (Ygf) in the southeastern part of the context area (Figure 26). The hand sample is a fine to medium-grained felsic granite, weathering to light olive-brown color. This sample exhibits a weak cleavage and is friable, and produces a distinct sandy texture when broken along cleavage planes. Visible phenocrysts include 5 to 7% dark biotite surrounded by light gray-colored reaction rims resembling plagioclase feldspar.

In thin section phenocrysts include ~50 to 60% quartz, 20 to 30% feldspar, 5 to 7% biotite and 2 to 4% opaque minerals, consistent with proportions seen in coarse granite. A crude to lightly-developed layering of phenocrysts is present (Figure 45 and Figure 46). Orientations of quartz and feldspar are random and do not exhibit any signs of foliated texture. Quartz and feldspar crystals have an equant or sub-rounded grain shape and exhibit a tightly packed texture, versus a texture of intergrown, interlocking crystals. Platy-shaped biotite mica phenocrysts, and possibly intergrown muscovite, are subparallel to grain layering, and appear to have grown between, around, and over grains, although they appear to be a constituent of primary layering. There does not appear to be any visible reaction rims on crystals in contact with biotite, which suggests biotite crystallized at the same time as other phenocrysts rather than replacing other crystals. Opaque minerals are also present as a constituent of layering.

Less common in thin section are several spherical-oblate or orbicular-shaped grains with rims of altered biotite (Figure 47). These “micro-orbicules” have oxidized or altered biotite rims. In one orbicule a subhedral plagioclase crystal (altered to sericite) has biotite concentrically wrapped around most of the plagioclase. Concentric spherules or orbicules were also observed in up to 30% of the hand sample, with concentric plagioclase (?) around biotite or opaque phenocrysts. Thus, based on hand sample and thin section, more than one variation of concentric mineralogy in an orbicule exists. Inclusions of quartz and sericite are common throughout the sample. Minor patchy chlorite mineralization was also present.

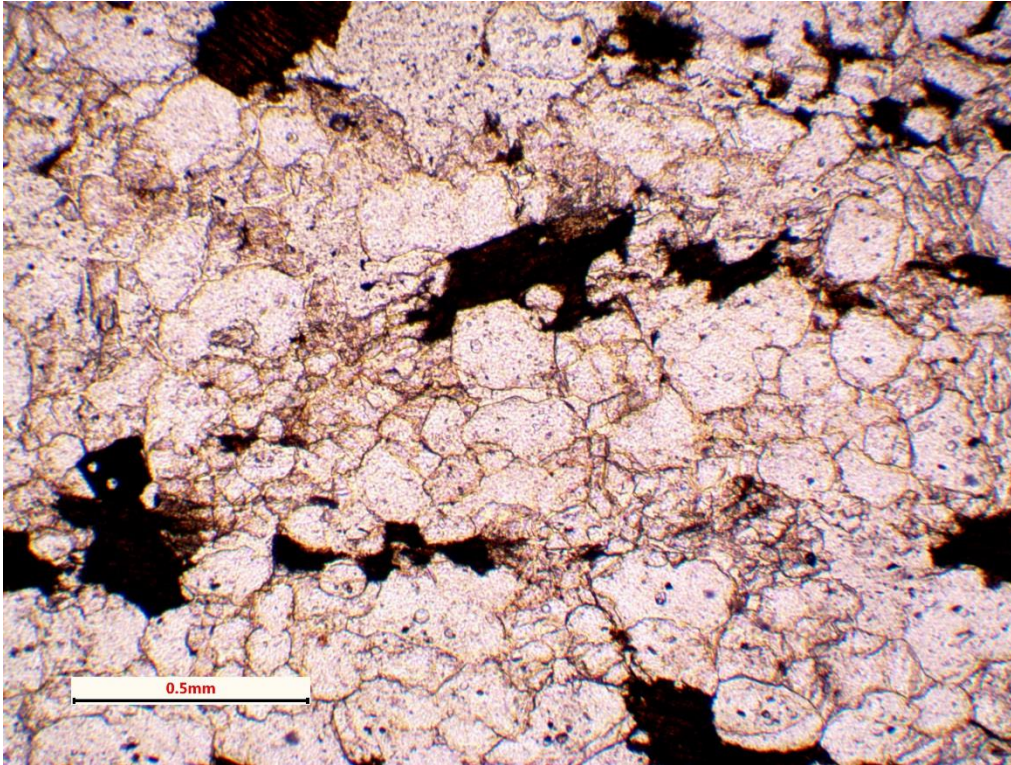


Figure 45. Sample P6 layering in plain-polarized light showing crude layering of phenocrysts. Dark phenocrysts are biotite mica. Clear phenocrysts of quartz and feldspar are outlined in very fine-grained mica. Layering of grains and cleavage in sample is horizontal in view. Scale in lower left is 0.5 mm wide.

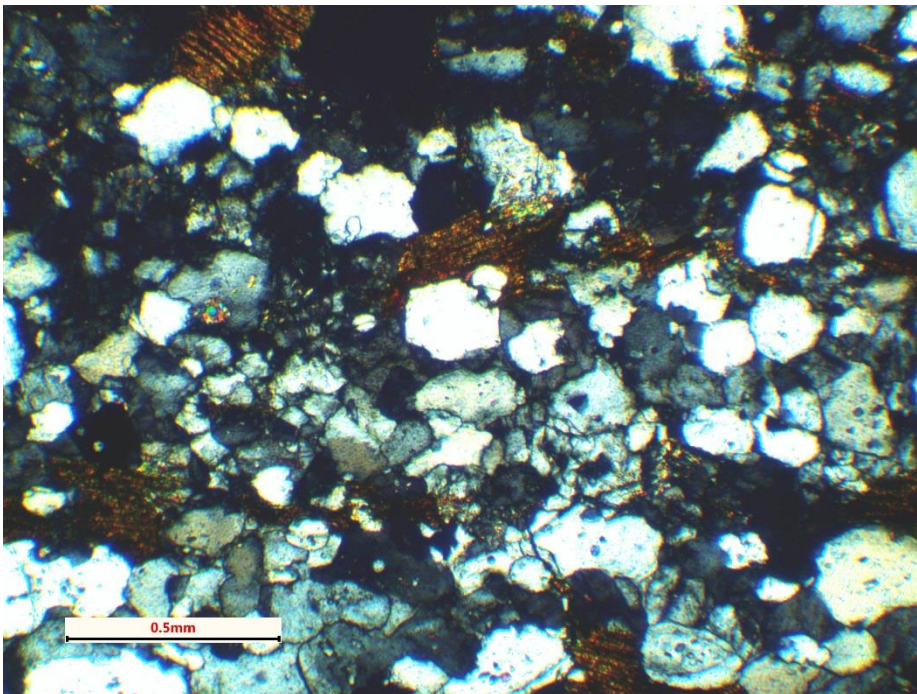


Figure 46. Sample P6 in same field of view as Figure 45, but in cross-polarized light. Gray and white phenocrysts are mostly quartz and feldspar. Notice sub-rounded to oblong shape of crystals. Scale in lower left is 0.5 mm wide.

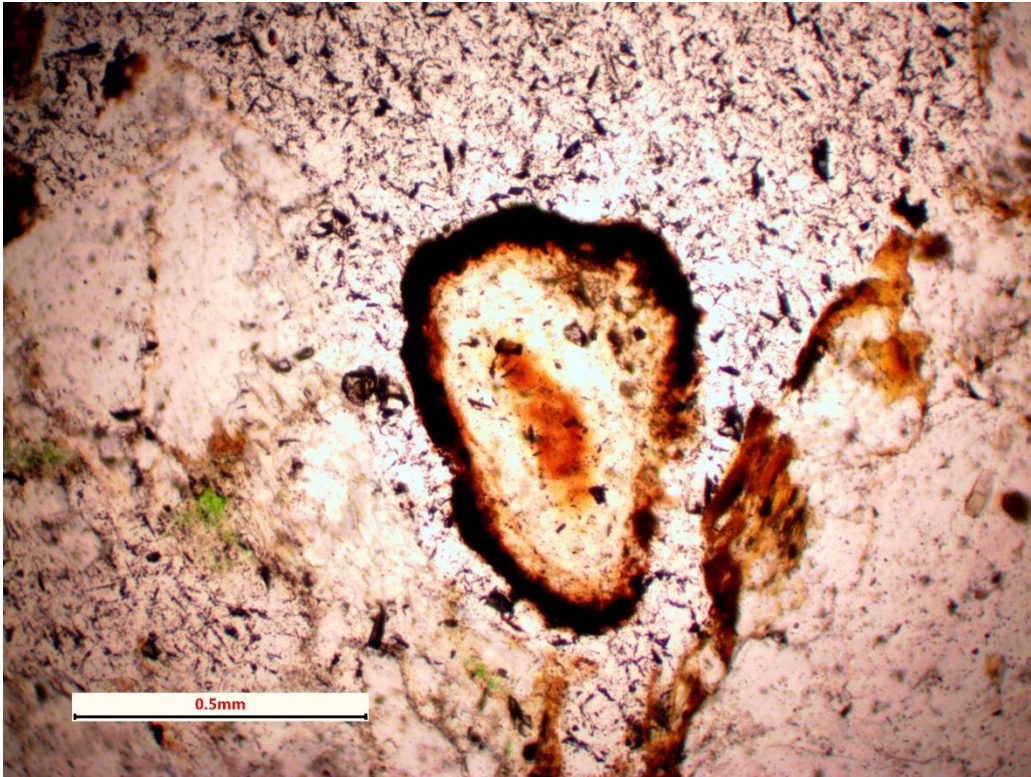


Figure 47. Sample P6 concentrically-laminated grain or “micro-orbicle” with a biotite (?) rim and unknown core composition. The black and white crystal hash is abrasive material used to make the thin section, a common erosional aspect of this rock when being prepared for thin sectioning. Green colored mineral is chlorite.

Sample P6 Interpretations

The relationship between fine-grained granite and other units in the map area is obscure due to poor exposure; however, it should be noted that an example of this unit was found in contact with orbicular granite at site P3. Finer-grained granite was also observed in a core and surrounding a single orbicule only a few meters from pegmatite at site P4 (Figure 35). Compared to coarse-grained granite the fine-grained texture is non-porphyritic, which suggests a different environment where crystals are cooling more uniformly and at faster rates than the main granite batholith.

The presence of concentrically laminated phenocrysts and layers of tightly packed sub-rounded phenocrysts suggest this sample is a cumulate, a type of rock exhibiting the gravitational or adhesive accumulation of crystals at the bottom of a magma chamber or boundary to solidified rock. The orbicular grains may suggest solid growth in a suspended, circulating melt prior to resting or adhering to a surface. Perhaps the orientation of layering in this rock can indicate the right-side-up orientation of granite; however, this may be an oversimplification without more detailed analysis of this map unit in the field.

The stand-alone orbicule shown in Figure 35 may be associated with a coarse sand-size crystalline cumulate formed in a fluid-rich environment. If the fine-grained portion in Figure 35 is a cumulate lithology, then the core and matrix are made of cumulate, suggesting portions of the cumulate are being reworked as orbicules. Some degree of recrystallization of quartz in Sample P6 did occur,

but the timing of this is not clear. Chlorite alteration is thought to post-date complete solidification of the rock.

3.3 Interpretations and Conclusions

Research of massive, milky quartz at Paraiso sheds light into the formation of such quartz and its accessory pegmatite minerals within the surrounding granite batholith. Unlike the milky quartz seen in older metamorphic rocks in the McDowell Mountains, the quartz and pegmatites at Paraiso represent a unique and rich opportunity to study the evolution of the Carefree granite in context to the rocks it intrudes.

The depth of emplacement of the granite batholith, pegmatites and milky quartz remains uncertain. In theory granite would have been completely crystallized at around 700 to 600 °C, although conditions and temperatures at which the pegmatites could continue to form were probably between 500 to 400 °C, possibly as low as 350 °C (Simmons and Webber, 2008). It is clear that the pegmatites represent a late-stage crystallization from a fractionated granite batholith.

Notably, the pegmatites in granite at Paraiso are only 0.5 to 1 km (0.3 to 0.7 miles) from older metamorphic rocks in the McDowell Mountains, which exhibit contact-metamorphism textures (Skotnicki, 2014). The presence of xenoliths commonly seen “floating” in the Paraiso-area granite, the apparent lack of radiating dikes away from the pegmatites, and the proximity of granite to metamorphic rocks in this area of the Preserve, suggests that the Paraiso pegmatites formed in a well-insulated and sealed environment at the margin of a large granite batholith (Figure 48).

Orbicular granite at Paraiso is interpreted to have formed from water- and vapor-rich circulating fluids during a late-stage of the batholith formation, prior to the formation of pegmatites and milky quartz that require a more stable environment. The orbicules themselves are cored with “digested” seed material derived from the main granite, and are overgrown by a shell of biotite and magnetite. Orbicules appear to have been largely solid before a granitic matrix crystallized the orbicules together. In addition to the orbicules, the finer-grained granite in one thin-section was found to have a cumulate texture, whereby crystals and miniature orbicules crystallized prior to settling out of a liquid melt. The formation of orbicules and cumulates is interpreted to have occurred prior to the last stage of crystallization, and also prior to relatively static conditions for the formation of granite pegmatite.

Granite pegmatite (including graphic granite and milky quartz) represents the final stages of crystallization of the Carefree granite, under thermal and magmatic conditions similar to granite formation but different geochemical conditions with limited (if any) circulation. Without a geochemical analysis the pegmatites at Paraiso cannot be adequately classified. The source of pegmatitic fluids are interpreted to be derived from residual granitic magma rather than a separate event of hydrothermal metamorphism of the granite. A universally accepted model for the genesis of pegmatites does not currently exist; but the crystallization of pegmatites from residual granitic melt is generally favored (Simmons and Webber, 2008).

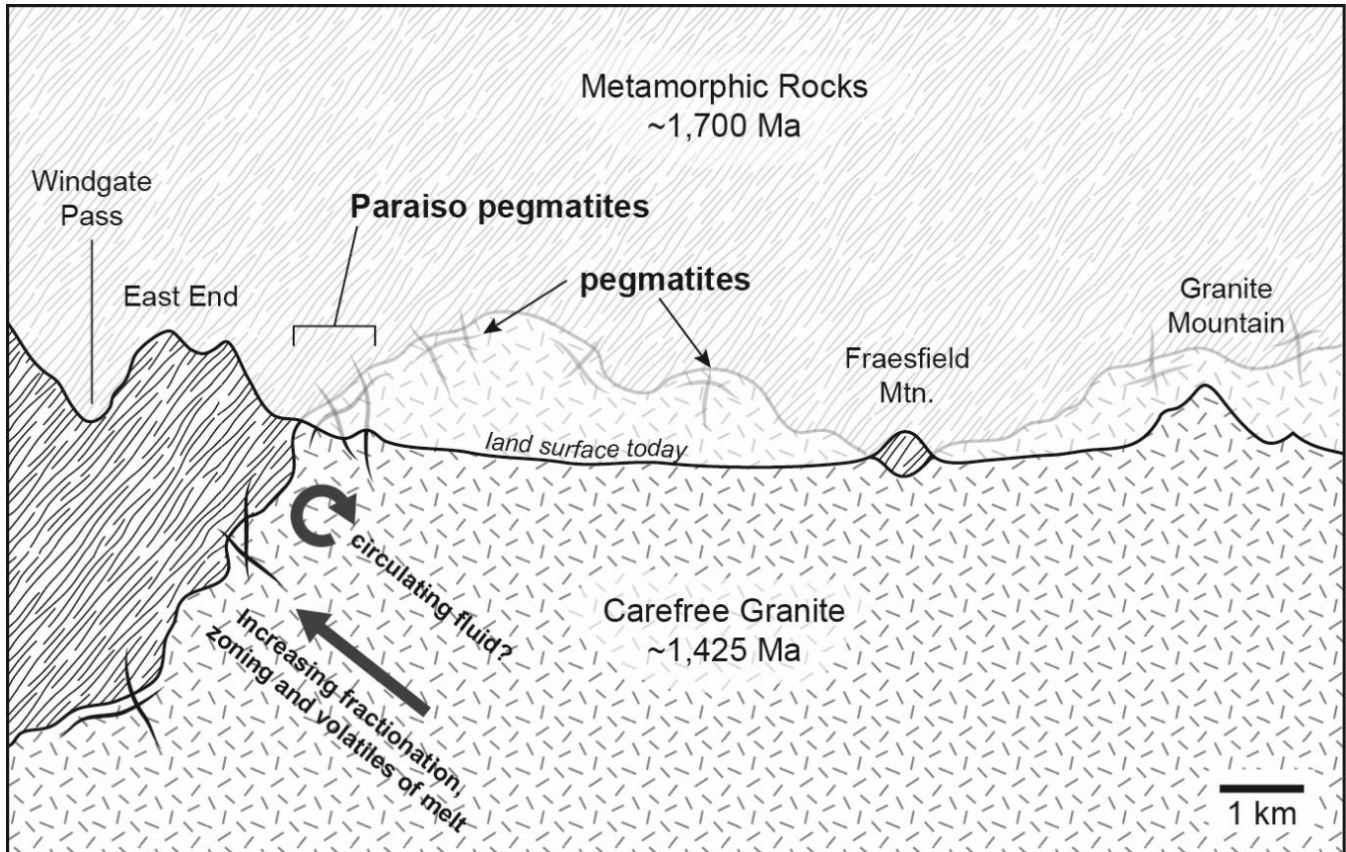


Figure 48. Conceptual diagram for the formation of granitic pegmatites during the late stages of the Carefree granite ~1,425 Ma. Pegmatites are thought to have grown relatively fast, but at temperatures relatively cooler than the interior of the granite batholith. Modern profile oriented south to north, left to right, facing west. Vertical exaggeration is ~4x. Orientation of metamorphic fabric and contact with granite overgeneralized. Shear zones and faults not projected. Fraesfield Mountain is assumed to be in its original position relative to the Carefree Granite and not faulted in to its present location.

Crystallization of tourmaline represents one aspect of intermediate crystallization, typically on the wall margin of massive quartz. Formation of tourmaline generates voluminous quantities of water and space filled with aqueous fluids, good conditions for pocket formation (London, 1986). Tourmaline is also present in large quantities along milky quartz veins hosted in metamorphic quartzite and schist in the Preserve, which may provide clues to quartz formation, fluid history, temperature and depth of formation under peak magmatic conditions. The presence of boron in tourmaline acts as a flux to decrease crystallization temperature and diffuse ions over a larger crystal-surface area, which allows for fewer and larger crystals to form (Simmons and Weber, 2008). Other flux elements that have the same effect include fluorine (F), phosphorus (P) and lithium (Li), which may be present in the Paraiso pegmatites.

In the case of pegmatites in general, the assumption that larger crystals grow more slowly in a slowly cooling magma has been shown not to be the case (Simmons and Webber, 2008). Although the temperature at which the pegmatites formed is not known, the large graphic granite, feldspar and quartz crystals (and perhaps orbicules and cumulate) probably crystallized much more quickly than the host granite, on the order of months to years. Thus, in this author's opinion, the position of pegmatites

near the margin of a granite batholith where temperatures are cooler and fracture-conduits are present would make sense.

Field mapping suggests the geometry of milky quartz and pegmatite are concentric rather than layered, although variations of both can be imagined (e.g. oblate lenses, tubular, etc.). In addition to the accessory minerals we observed (e.g. tourmaline and magnetite), other accessory minerals are likely present. Accessory minerals typically associated with pegmatites in the region (Morning Star Mine, Bull. 180; Jahns, 1952) include spodumene, amblygonite, lepidolite, cassiterite, apatite, garnet and beryl.

Although evolution of the Carefree granite and its margins are not well understood, a conceptual model for the formation of pegmatites can include increasing degrees of fractionated melt towards the margin of the batholith, consistent changes in mineral chemistry from the wall to core within pegmatites, increasing volatiles and rare elements, and increasing zoning (Simmons, and , 2008). Closely related to the emplacement of the Carefree granite both spatially and temporally, may be multiple generations of granite intrusion, further complicating a general model for pegmatites.

Based on our findings we interpret the pegmatites (which includes the core of milky quartz) at Paraiso to represent the final stages of crystallization of the Carefree granite. Given the presence of orbicular granite, cumulates, and zoned pegmatites with quartz cores, we interpret the range of grain size, various textures and compositions to represent a fractionated granite melt, with a complex and inconsistent cooling history. Pegmatite fluids are interpreted to be a fractionated residual melt of the Carefree granite, have low viscosity, be H₂O rich, alkali-rich, and potentially rich in trace and other elements.

Based on our observations, mapping, and analysis of rock samples, the following sequence of events are interpreted to have occurred at Paraiso:

1. 1,750 to 1,650 Ma: Deposition of sedimentary rocks, followed by rapid burial, compaction and cementation.
2. 1,700 to 1,600 Ma: Metamorphism of pre-existing sedimentary rocks during the Mazatzal Orogeny with peak metamorphism occurring around 1,650 Ma.
3. 1,425 Ma (?): Emplacement of the Carefree granite batholith in multiple stages:
 - a. Early-stage of granite emplacement: granite batholith(s) are mechanically "injected" into surrounding rock. Formation of the batholith may have occurred at depths ranging from 3 to 10 km (?), and temperatures from 800 to 1,200 °C. Dome-like cupolas and roof pendants stoped from older igneous and metamorphic rocks are found as xenolith inclusions in the granite at Paraiso.
 - b. Intermediate-stage circulating: fluid-rich, low viscosity magma forms orbicular granite and cumulates. Orbicules and cumulate deposits may have formed in a closed system to allow reworking of solidified granite as seed material for orbicules, and new crystallization to be circulated or moved in a fluid environment.
 - c. Late-stage pegmatite growth: magma fluids collected in a closed system in oblate-shaped pegmatite bodies. Residual magma fluids crystallized sequentially inward into mineral zones in a stable yet delicate thermal and chemical balance. Cores of milky quartz represent final crystallization of the pegmatite. Pegmatite minerals likely

grew below 600 °C, to as low as 350 °C, under confining pressures sufficient to prevent major escape of volatile components during giant-crystal growth. Accessory minerals include tourmaline and magnetite, although many other accessory and rare minerals may be present in any given pegmatite body.

- d. End-stage replacement and alteration: Small cavities, or miaroles, remaining in the pegmatite were present, where crystals grew and terminated in open cavities. Portions of the pegmatites may have undergone sericite, chlorite and sulfide alteration.
4. 1,400 Ma or 1,100 Ma: Low-grade metamorphic conditions are present, either related to waning stages of Carefree magmatism post 1,425 Ma, or related to the Grenville Orogeny around 1,100 Ma (Bright et al., 2014). Shear zones cross-cut granite in close proximity to Paraiso. Low-grade hydrothermal conditions may have produced alteration textures along fractures, such as chlorite and epidote.
5. 25 to 15 Ma: Extension related to the Mid-Tertiary Orogeny and Basin and Range events produced northwest-southeast joints in the region. Oxidation of iron-bearing minerals at shallow depths and temperatures are present throughout Paraiso.

4.0 Implications and Next Steps

4.1 Implications for and Applicability to Other Quartz Veins Outcrops

Based on this study, it is apparent that quartz veins in the Preserve have formed over a period of approximately 300 to 600 million years in a range of tectonic, magmatic and hydrothermal environments. This period relates to metamorphism during the Mazatzal Orogeny around 1,650 million years ago, plutonism around 1,400 million years ago, and tectonism around 1,100 Ma during the Grenville Orogeny.

The majority of quartz veins are hosted in Paleoproterozoic metamorphic rocks. For those veins we interpret the deep-seated and low grade regional metamorphism associated with the Mazatzal Orogeny to have generated widespread conditions ideal for the growth of milky quartz veins. Based on previous studies and research during this study, the primary source of quartz veins seen throughout meta-sedimentary rocks in McDowell Mountains does not appear to be directly related to granitic plutons or mafic intrusions.

However, this does not preclude *new* quartz growth or secondary growth related to thermal halos generated from such heat sources. The relationship between plutonic rocks intruding older meta-sedimentary rocks is one area for future research. It is possible that quartz veins were formed during later magmatic and tectonic events related to the Laramide (~100 to 80 Ma) and mid-Tertiary (~25 to 15 Ma) Orogenies, although we suspect these intrusions to have occurred at relatively shallow depths with localized contact metamorphism.

4.2 Additional Research Questions

Paraiso

The diverse geology at Paraiso offers an excellent opportunity to study the geochemistry and phases of the Carefree batholith adjacent to the older country rock. Further detailed mapping of mineral species, mineral associations and mineral zones is needed, followed by geochemical analysis. Geochemical analysis of bulk chemistry, trace elements, and rare earth elements will expand our understanding of the type of pegmatite, the range of depth and temperature in which it formed, and the sequence of fractionation. Results from this study and future work may have implications associated with the Carefree granite and perhaps other 1,400 Ma granites found the Preserve and surrounding area.

Fraesfield

The geology at Fraesfield is represented by three distinct geologic events: deposition and metamorphism of pre-existing rocks, intrusion of the Carefree granite, and subsequent shearing of all rocks. Further work to characterize the formation, deformation and reformation of quartz can focus on specific associations of quartz and its host rock, for example, the study of relatively non-deformed quartz veins at a mesoscopic scale within granite or quartzite, or quartz veins specifically associated with extensive narrow mylonite zones (e.g. East End mylonite). It would also be possible to analyze zircon grains within quartzite to determine the age of the source rocks for the quartzite sandstone.

Other Quartz Veins

Since milky quartz veins are abundant in meta-sedimentary rocks in the Preserve, collecting a sample from two or three separate outcrops for thin-section and fluid inclusion analyses may yet reveal well-preserved fluid inclusions which formed in representative environments. Additional research could also determine if there is a relationship between milky quartz in metamorphic rocks to any surrounding granites. For example, the abundance, size and shape of quartz veins compared to the distance from the nearest granite could be mapped or documented at a mesoscopic scale. This may provide insight into whether quartz veins in metamorphic rocks formed as a partial melt within a thermal halo generated by surrounding granite(s).

The preliminary analysis to select sites for review, described in section 1.2.1, identified several previously unknown quartz outcrops in the Preserve. These observations could be verified by field investigations and, if valid, be entered into existing geologic survey maps of the Preserve.

Acknowledgements

The authors would like to thank the entire City of Scottsdale Preservation staff including Preserve Director Kroy Ekblaw, Preserve Manager Liz Hildenbrand, Senior Planner Scott Hamilton, plus Rob Chasan in the Information Technology department for their ongoing assistance. This research work was completed under and performed in accordance with a permit from the City of Scottsdale. Without a research permit issued by the City of Scottsdale, off-trail travel and removal of items from the Preserve are strictly prohibited and punishable by law.

We also would like to thank McDowell Sonoran Field Institute Manager Melanie Tluczek and McDowell Sonoran Conservancy Executive Director Mike Nolan for their leadership and support of this project.

Thanks to Nick Rowe and Jim Reynolds for their time spent reviewing thin sections and providing valuable input and information related to the formation of milky quartz features. AZGS Tucson geologists provided valuable input, review and equipment for thin section analysis. Nyal Niemuth with AZGS in the Phoenix office provided context and support for previous studies, and use of the XRF Analyzer, Geiger counter and UV lamp. Steve Skotnicki provided valuable input and context related to his many years' experience mapping in the area.

Finally, we especially want to acknowledge the hundreds of hours of photography and field work, data entry, organization, and mapping performed by MSFI volunteers in support of this project. This work would not have been possible without the participation of Bobby Alpert, Con Englehorn, Franco Farina, Jim Frier, Thomas Hartley, Marianne Jensen, Ralph Lipfert, John McEnroe, Joni Millavec, Bill Ruppert, Megan Stump, and Kathy Ann Walsh. The granite in the Fraesfield shear zone and the orbicular granite at the Paraiso site – both important for interpretation of the sites – were first noted by MSFI volunteers, who recognized their significance. All photomicrographs are by Brian F. Gootee. All other photographs are by members of the project team.

References Cited

- Affholter, K.A. and Lambert, E.E., 1982, Newly Described Occurrences of Orbicular Rock in Precambrian Granite, Sandia and Zuni Mountains, New Mexico. New Mexico Geological Society Guidebook, 33rd Conference, Albuquerque Country II, pp. 225-232.
- Brace, W.F. and Kohlstedt, D.L., 1980, Limits on Lithospheric Stress Imposed by Laboratory Experiments. *Journal of Geophysical Research*, Vol. 85, No. B11, pp. 6248-6252.
- Bright, R.M., Amato, J.M., Denyszyn, S.W., and Ernst, R.E., 2014, U-Pb geochronology of 1.1 Ga diabase in the southwestern United States: Testing models for the origin of a post-Grenville large igneous province. *Geological Society of America, Lithosphere*, doi: 10.1130/L335.1, 23 p.
- Couch, N.P., 1981, Metamorphism and Reconnaissance Geology of the Eastern McDowell Mountains, Maricopa County, Arizona. Unpublished Master's Thesis, Arizona State University, 56 p.
- Christenson, G.E., Welsch, D.G., and Péwé, T.L., 1978, Environmental Geology, McDowell Mountains Area, Maricopa County, Arizona, Arizona Geologic Investigation Folio GI-1, scale 1:24,000.
- Doe, M.F., Jones, J.V., III, Karlstrom, K.E., Thrane, K., Frei, D., Gehrels, G., and Pecha, M., 2011, Basin formation near the end of the 1.60-1.45 Ga tectonic gap in southern Laurentia: Mesoproterozoic Hess Canyon Group of Arizona and implications for ca. 1.5 Ga supercontinent configurations: *Lithosphere*, v. 4, n. 1, p. 77-88.
- Fenn, P.M., 1986, On the origin of graphic granite. *American Mineralogist*, Volume 71, pp. 325-330.
- Gillentine, J.M., Karlstrom, K.E., Parnell, R.A., Jr., and Puls, D.D., 1991, Constraints on temperatures of Proterozoic metamorphism in low-grade rocks of central Arizona, *Arizona Geological Society Digest* 19, p. 165-180.
- Isachsen, C.E., Gehrels, G.E., Riggs, N.R., Spencer, J.E., Ferguson, C.A., Skotnicki, S.J., and Richard, S.M., 1999, U-Pb geochronologic data from zircons from eleven granitic rocks in central and western Arizona. *Arizona Geological Survey Open File Report, OFR-99-05*, 27 p.
- Jahns, R.H., 1953, The Genesis of Pegmatites, Occurrence and Origin of Giant Crystals. *The American Mineralogist*, Vol. 38, No. 7 and 8, pp. 563-598.
- Jahns, R.H., 1952, Pegmatite deposits of the White Picacho District, Maricopa and Yavapai Counties, Arizona. *University of Arizona Bulletin, Arizona Bureau of Mines, Bulletin* 162, 105 p.
- Karlstrom, Karl E. and Bowring, Samuel A., 1991, Styles and timing of Early Proterozoic deformation in Arizona: Constraints on tectonic models, in Karlstrom, Karl E., editor, *Proterozoic Geology and Ore Deposits in Arizona, Arizona Geological Society Digest* 19.
- Levenson, D. J., 1966, Orbicular rocks: A review: *Geological Society of America Bulletin*, v. 77, p. 409-426.
- London, D., 1986, Formation of tourmaline-rich gem pockets in miarolitic pegmatites. *American Mineralogist*, Volume 71, pp. 396-405.

- Lund, K., Box, S.E., Holm-Denoma, C.S., San Juan, C.A., Blakely, R.J., Saltus, R.W., Anderson, E.D., and DeWitt, E.H., 2015, Basement domain map of the conterminous United States and Alaska: U.S. Geological Survey Data Series 898, 41 p., <http://dx.doi.org/10.3133/ds898>.
- Nyman, M.W., Karlstrom, K.E., Kirby, E., and Graubard, C.M., 1994, Mesoproterozoic contractional orogeny in western North America: Evidence from ca. 1.4 Ga plutons: *Geology*, v. 22, p. 901-904.
- Péwé, T.L., Bales, J. and Montz, M., 2012, Reconnaissance Environmental Geology Maps of Northern Scottsdale, Maricopa County, Arizona. Arizona Geological Survey Contributed Map (CM) 12-B, 3 map sheets, map scale 1:24,000. (From unpublished maps compiled in 1983).
- Simmons, Wm. B. and Webber, K.L., 2008, Pegmatite genesis: state of the art. *Eur. J. Mineral*, 20, 421-438.
- Skotnicki, J. S. and Leighty, R.S., 1998, Geologic Map of the Maverick Mountain 7.5' Quadrangle, Maricopa County, Arizona. Arizona Geological Survey Open File Report, OFR-98-14, 1 map sheet, map scale 1:24,000, 18 p.
- Skotnicki, J. S., 1996, Geologic Map of Portions of the Fort McDowell and McDowell Peak Quadrangles, Maricopa County, Arizona. Arizona Geological Survey Open File Report, OFR-96-11, 1 map sheet, map scale 1:24,000, 20 p.
- Skotnicki, S. J., Leighty, R.S., and Pearthree, P.A., 1997, Geologic Map of the Wildcat Hill Quadrangle, Maricopa County, Arizona. Arizona Geological Survey Open File Report, OFR-97-02, 1 map sheet, map scale 1:24,000, 17 p.
- Vance, B., 2012, Structural Evolution of the McDowell Mountains Maricopa County, Arizona. Unpublished Masters Thesis, Arizona State University, 124 p. Found at <http://hdl.handle.net/2286/R.A.97688>.
- Wessels, R.L., and Karlstrom, K.E., 1991, Evaluation of the tectonic significance of the Proterozoic Slate Creek shear zone in the Tonto Basin area, in Karlstrom, K.E., ed., *Proterozoic geology and ore deposits of Arizona*: Arizona Geological Society Digest 19, p. 193-210.

Glossary of Geologic Terms

Accessory mineral	Accessory minerals generally occur in minor amounts. Their presence or absence is incidental to the basic identification of the rock.
Alluvial deposit (alluvium)	Sediment transported and deposited downslope by running water from ephemeral precipitation events.
Alteration	A change in mineral composition caused by physical or chemical means, especially by the action of hydrothermal (see definition) solutions.
Anhedral	Crystals without distinct faces. Contrast with euhedral (see definition).
Anticline	A fold that is convex-up (i.e. opens downward) and has its oldest layers at its core. The layers dip down away from the center of the fold.
Augen	Eye-shaped mineral grains or rock fragments formed during foliation of a rock and visible in some foliated metamorphic rocks.
Autolith	An inclusion of previously crystallized igneous rock that is surrounded by igneous rock that crystallized later from the same magma.
Basalt	Extrusive volcanic (igneous) rock relatively poor in silicon dioxide (silica), usually fine-grained due to rapid cooling at the surface.
Batholith	A large emplacement of intrusive igneous rock formed from cooled magma.
Bearing	In navigation, bearing is the angle between true north and a line going from the current position to another defined object or position, expressed in degrees from 0 to 360. For example, an object due east of the current location would have a bearing of 90 degrees.
Bedding	A distinct layer in a rock defined by well-defined planes at the top and bottom. Bedding layers usually are sedimentary in origin.
Bedrock	Consolidated native rock exposed at the surface in outcrops or concealed under sediment or water.
Biotite	Sheet silicate mineral in the mica group; often dark-colored.
Brittle deformation	Deformation of brittle rock by fracturing (see definition) or breaking.
C-axis of quartz	The ideal crystal shape of quartz is a six-sided prism with six-sided pyramids at each end. The c-axis connects the tips of the two pyramids at the ends of the crystal. Usually, this is the longest axis of a quartz crystal.
Cataclastic rock	Metamorphic rock formed by the brittle fracturing of the original rock and further reduction in particle size through crushing and grinding, usually associated with fault zones.
Chlorite	Chlorites are a large family of common metamorphic minerals, often green in color; chloritization is the process of forming chlorite mineralization
Colluvial deposit (colluvium)	Loose sediment transported and deposited downslope by gravity.
Colluvial lag	A coarse deposit of colluvium (see definition) left behind after finer-grained material is removed by erosion.
Competent rock	Rock that is relatively resistant to erosion or deformation.
Contact	An identifiable boundary between different types of rock or sediment. A contact can also be structural, a fault for example.

Crenulation or crenulation cleavage	Small-scale folding (a few millimeters in wavelength) in metamorphic rocks. Crenulation forms when a new stress direction and the associated cleavage or foliation is superimposed on an older one. In mica rocks, crenulation may occur as “kink bands” (see definition).
Cross-bedding	A sedimentary structure in which several rock layers are “stacked” at slight angles to the horizontal and to each other. The individual, inclined layers also may be called cross-beds.
Cumulate	Cumulate rocks result from the gravitational settling of solid crystals within magma.
Decrepitation	The disintegration of a mineral grain or explosion of a fluid inclusion, often violently, upon heating.
Dike	An intrusion of magma into pre-existing rocks that cuts across rock bodies.
Diorite	An intrusive, coarse-grained igneous rock consisting mostly of plagioclase feldspar (see definition) and mafic minerals (see definition), with little quartz.
Dip	The maximum angle of decline of a tilted layer relative to a horizontal plane, expressed as a dip <i>angle</i> between 0 and 90 degrees. The dip <i>direction</i> is the direction of steepest declination on the tilted feature, i.e. the direction in which water would run down the feature. By definition, the dip direction is 90 degrees clockwise from the strike direction.
Double-bubble texture	A gaseous bubble surrounded by a liquid bubble, both represented in a single fluid inclusion.
Ductile deformation	Deformation without breaking; plastic deformation without fracturing.
Eolian	Pertaining to the wind, for example, erosion and deposition of sedimentary material by the wind.
Equant	Refers to crystals or mineral grains of roughly equal size in all directions.
Equigranular	Composed of crystals or mineral grains of approximately the same size.
Euhedral crystal	Crystals with well-formed faces, usually flat with sharp outlines. Contrast with anhedral (see definition).
Extrusive (igneous rock)	Volcanic rock formed when magma solidifies at or near the surface, cooling relatively quickly and resulting in limited (or no) crystal formation.
Fault	Fracture or break in originally continuous rock with relative displacement or separation of one side from the other.
Feldspar or Plagioclase feldspar	Feldspars are a large family of related minerals consisting of aluminum silicates combined with potassium, sodium, or calcium; plagioclase feldspar contains only sodium or calcium, not potassium.
Felsic minerals	Silicate minerals that are rich in lighter elements such as silicon, aluminum, and potassium. Felsic minerals often are light-colored. Quartz and potassium feldspar are felsic minerals. Contrast with mafic minerals (see definition).
Fissile	Easily split into thin sheets, a common property of foliated metamorphic rocks.
Fold	Bent or folded layers of rock, usually under plastic or ductile conditions. Folds have limbs which are joined along a hinge. The limbs of a fold are separated by an axial surface (which may be flat or curved depending on the fold).

Foliation	Planar texture or fabric in rock, often associated with the flattening or alignment of mineral grains due to compressive stress and/or shearing of the original rock under metamorphic conditions.
Fractionation or fractionated material	A process of phased crystallization of magma. The result of each crystallization phase is a residual fluid of different composition than the one preceding it. This results in each phase of crystallization from the residual fluid having a different composition than the previous one.
Fracture	A break in originally continuous rock due to brittle deformation.
Geobarometry and geothermometry	Geobarometry is measurement of the pressure under which a metamorphic or intrusive igneous rock was formed. Geothermometry is measurement of the temperature at which such a rock was formed.
Granitic rock	Granite-like rock, i.e. generally light-colored, coarse-grained plutonic rock containing abundant quartz and feldspar, with other minor minerals.
Hinge line	The line of maximum curvature (i.e., minimum curve radius) along a fold. In a U-shaped fold, for example, the hinge line is along the bottom of the U perpendicular to the direction of the fold. The hinge line orientation is described in 3-dimensional space with an azimuth (equivalent to strike or compass bearing) and a dip (angle of the hinge line below horizontal). The hinge line lies on the axial surface, which separates the two sides or limbs of a fold. "Fold axis", sometimes used interchangeably, actually means something different.
Hydrothermal activity	Activity relating to hot (sometimes superheated) water, often associated with volcanic or magmatic activity.
Igneous rock	Rock produced by the cooling and solidification of molten rock (magma), either on the surface as extrusive volcanic rock or below the surface as intrusive plutonic rock.
Immature (rock)	A sedimentary rock which lacks a separation of minerals and constituents from its parent rock which it came from, usually characterized by poorly-sorted grains, angular grains, unstable minerals, and weathered minerals.
Incompetent rock	Rock that is relatively poor at resisting erosion or deformation.
Joint	Rock fracture where the opening between the sides of the joint is greater than the lateral displacement between the sides of the joint. Compare with "fault".
Kink, kink fold, or kink band	A fold with sharp hinges and flat sides formed in semi-brittle to semi-ductile environments. For example, V-, W-, or Z-shaped folds are kinks. Kink bands sometimes refer to broader bands of material with zigzag edges. See "crenulation".
Laminae	The thinnest recognizable layer in sedimentary rock, commonly 0.05 to 1 mm thick.
Laths	Long, thin crystals.
Lenticular	A feature that is thick in the middle and thin at the ends. Augens and pegmatite bodies are commonly lenticular in shape.
Lithology	A description of the obvious physical characteristics of a rock or rock unit examined visually or with low magnification, such as color, mineral content and grain size.
Magmatic or magmatism	Geologic activity involving magma (molten rock).

Mafic minerals	These are silicate minerals that are rich in magnesium and iron. Mafic minerals often are dark-colored. Biotite is a mafic mineral.
Magmatic water and meteoric water	Magmatic water is the water content within magma. Magmatic water may be released to the atmosphere in volcanic eruptions and also may be released underground as hydrothermal fluids. Meteoric water is derived from precipitation and infiltrated as groundwater in the shallow subsurface.
Mega-crystic	Having very large, generally euhedral (see definition) crystals.
Mesosopic	A qualitative term used to describe an observation on a scale between naked-eye visibility and outcrop-size. The prefix meso- often denotes intermediate in size between micro- and mega-.
Metamorphic or Metamorphosed Rock	Rock produced by metamorphic conditions, i.e. heat and pressure sufficient to cause physical and/or chemical changes in the original rock but not sufficient to melt the rock into magma.
Miarolitic cavity	Irregularly-shaped cavities in rock, often filled with crystals made of the minerals present in the surrounding rock. Commonly found in granitic pegmatites and other intrusive igneous rocks.
Mica or Micaceous	Consisting of or containing mica (a family of sheet-like silicate minerals) or resembling mica, usually in being thinly foliated; mica is a common alteration mineral in plagioclase feldspar in areas that have been subjected to hydrothermal alteration
Mica fish	Elongated mica crystals that often are used to determine the sense of shear (see definition).
Mica-schist	Schist is a crystalline metamorphic rock composed of more than 50% tabular and elongated minerals with grains visible to the naked eye. Nearby grains usually are parallel. Schists tend to split into layers. Schists often are named for the main minerals in them, so mica-schist contains mainly mica and quartz.
Microcline/albite feldspar	Varieties of feldspar. Microcline is rich in potassium while albite is rich in sodium. Crystals of these two types of feldspar often grow together in a configuration called synthetic or polysynthetic twinning (see definition).
Mineralization	The process of generating new minerals in a rock, usually from hydrothermal deposition or regional metamorphism. The word also can refer to the deposits of minerals that result from this process, e.g., quartz deposits may be mineralized (contain minerals) as a result of mineralization.
Minerals	Minerals are the basic building blocks of rocks. Rocks usually are aggregates of different minerals, each of which has characteristic chemical composition and physical properties.
Monocrystalline or uniaxial	A single crystal in which the crystal lattice of the entire sample is continuous and unbroken.
Mylonite	Rock that has been deformed plastically (ductilely) by crushing or grinding of rock grains and without fracturing; often indicating a ductile shear zone. Mylonitized rock exhibits this form of ductile deformation.
Orogenesis	Process of forming mountain ranges by deformation of the Earth's crust.
Outcrop	Bedrock exposure at the surface.
Overprinting	The superposition of new structural features over older ones.

Overtured bedding	In overturned beds the stratigraphic top of the beds are lower than the stratigraphic bottom, where strata in sedimentary bedding have been rotated more than 90 degrees vertically from their original horizontal positions.
Paleoproterozoic	Between 2,600 and 1,600 million years ago.
Pegmatite	A descriptive term for igneous rock, usually similar in composition to granite, consisting almost entirely of interlocking crystals more than 3 cm in length. A rock with this composition is called pegmatitic.
Petroscope or petrographic microscope	A type of optical microscope used to identify rocks and minerals in thin sections. Petroscopes usually have rotating stages on which specimens are mounted and the ability to polarize the light passed through the specimen to the eyepiece.
Phenocryst	A visible crystal surrounded by a finer-grained groundmass in an igneous rock. A rock with phenocrysts is called a porphyritic igneous rock.
Plutonic (or intrusive) rock	Rock formed from magma cooling slowly beneath the surface, composed of coarse-grained crystals visible to the naked eye.
Polarity	The direction in which electromagnetic waves passing through a material are polarized. A single polarity (rather than multiple polarities indicating several different directions of polarization) may indicate a uniform crystal structure.
Polycrystalline	Composed of crystals of the same variety but different sizes, shapes and orientations.
Porphyritic rock	Igneous rocks containing crystals of obviously different sizes.
Protolith	The original rock from which a metamorphic rock is formed. For example, sandstone is the protolith of quartzite.
Pseudomorph	A secondary mineral that has replaced the original material and retained the crystal form of the original.
Quartz	An abundant, hard, and stable mineral composed of crystalline silicon dioxide. Pure quartz is colorless and translucent, but slight impurities produce colored varieties of quartz. Milky quartz results from fluid inclusions trapped during crystal formation.
Quartz wedge	An optical accessory used in polarized-light microscopy.
Quartzite	Metamorphic rock produced from quartz-rich sandstone. Quartzite resists erosion and deformation and therefore is a "competent" rock. It usually is white to gray but colored varieties exist due to impurities such as iron.
Recrystallization	A metamorphic process under elevated heat and/or pressure in which the atoms of an existing crystal are reorganized, often by being packed closer together, to create a new crystal structure. The new crystals typically are larger than the original ones.
Retrograde minerals	As metamorphic rock cools and is subject to decreasing pressure, some of the chemical reactions and physical rearrangements that took during initial burial (with the attendant heating and increasing pressure) may partially reverse. Minerals that combined and disappeared during metamorphism may partially reappear as the metamorphic rock moves toward the surface, especially if carbon dioxide and/or water are present. These reappearing minerals are called retrograde minerals and the process is retrograde metamorphism.

S-fold/Z-fold	S and Z describe the appearance of multiple small folds viewed from the side (so the limbs and hinges are visible). Imagine a bedding layer in a rock as a sheet of paper held horizontally in front of you. If you move your <i>left</i> hand to the right and upward (i.e., clockwise) relative to your right hand, the sheet of paper bends into a Z-shape. If instead you move your <i>right</i> hand to the left and upward (i.e., anti-clockwise) relative to your left hand, the paper bends into an S-shape. The shape of folds can indicate the shear sense, the direction in which the shear acted along the top and bottom of the fold.
Schist	See “mica-schist”
Sense of Shear	Shearing is strong deformation in a limited area of rock (the shear zone) surrounded by areas with less deformation. The sense of shear describes the relative movement of rock within a shear zone when viewed from above. In dextral (right-lateral) shear there is a clockwise sense of rotation between the two sides of the shear zone. There is a counter-clockwise sense of rotation in sinistral (left-lateral) shear.
Sericite	Sericite is a very fine-grained mica. It is a common alteration mineral (see definition) of feldspars in areas exposed to hydrothermal activity (see definition). Sericitization refers to the hydrothermal or sometimes metamorphic process that leads to the introduction of sericite or the alteration or replacement of material (typically feldspar minerals) by sericite,
Shear zone	A planar or tabular body of sheared rock.
Silicate	Rock consisting primarily of minerals composed of combinations of silicon and oxygen with other elements.
Slope creep	Slow downward movement of surface material on a slope.
Sphene	Also called titanite, this is a calcium titanium silicate that is a common accessory mineral in granitic and similar igneous rocks and associated pegmatites. It also occurs in metamorphic rocks including schists.
Spheroidal weathering	A form of chemical weathering in which concentric shells of decayed granite are successively loosened and separated from unweathered portions of the granite.
Stope	An underground excavation from an overlying ceiling of rock.
Stratigraphy	The study of rock or layered strata, their relative position or order, and their age.
Stylolite	An irregular, interlocking contact between two rock surfaces. This is not a fracture but rather an area where minerals have dissolved under pressure and the remaining mineral grains have been compacted.
Strike	The strike direction of any tilted layer or planar feature is the line showing the intersection between the layer or planar feature and a horizontal plane, described as an angle from 0 to 360 degrees relative to true north. By definition, the strike direction is 90 degrees anti-clockwise from the dip direction.
Subaerial	Immediately adjacent to or on the land surface.
Subhedral	Crystals partly bounded by obvious faces. Intermediate between euhedral and anhedral (see definitions).
Sub-parallel	Almost parallel.

Subsolidus conditions	Conditions in which a rock or mineral is in a state between being completely solid and completely melted. Similar to a ductile or plastic state.
Synthetic or polysynthetic twinning	Twinning occurs when two different crystals inter-grow in a pattern. Microcline and albite feldspar (see definition) inter-grow in what looks like a repeated grid pattern when a thin section of rock containing these minerals is observed microscopically.
Top-to-the-(direction)	The orientation of upright bedding preserved by sedimentary structures such as cross-bedding (see definition).
Tourmaline	A crystalline boron silicate mineral, often referred to as schorl. Black tourmaline sometimes is found in granite and granite pegmatite (see definition), often as deposits of very thin, long crystals with triangular cross-sections.
Transposed plane	A younger foliation plane that has replaced an older one due to stronger deformation. Transposed planes are evidence for multiple deformation events.
Trough cross-bedding	Cross-beds that have curved (rather than planar) lower surfaces.
Undulose extinction	This is a property of certain minerals when examined in thin section under polarized light. As the specimen is rotated, individual mineral grains appear black when the polarization due to the mineral blocks all light from passing through. The blockage of transmitted light is called extinction. If a mineral is deformed ductilely, the crystal lattice may warp. This means that different parts of a crystal may cause extinction at different angles of rotation. The result is waves of blackness crossing the face of a specimen as it is rotated.
Uniaxial	Having a single optical axis when viewed under polarized light in a petroscope (see definition).
Vein	A generally sheet-like deposit of mineral(s) found filling a joint or fracture that cuts across a rock, usually by precipitation from an aqueous solution.
Xenocryst	A crystal that is foreign, i.e., of different origin, than the rock in which it occurs.
Zircon	Zircon is an extremely stable zirconium silicate. It is very hard (harder than quartz) and chemically inert, so it persists once formed. It is a common accessory mineral in igneous and metamorphic rocks. Because zircons contain trace amounts of uranium and thorium, they can be dated based on the radioactive decay of uranium to lead

Primary Sources:

1. A Dictionary of Geology and Earth Sciences, edited by Michael Allaby, published by the Oxford University Press, 2013.
2. Dictionary of Mining, Mineral, and Related Terms, published by the American Geological Institute, 1997.
3. General Dictionary of Geology, by Alva Kurniawan, John McKenzie, and Jasmine Anita Putri, published by the Environmental Geographic Student Association, 2009.
4. Guide to Rocks and Minerals, by Annibale Mottana, Rodolfo Crespi, and Giuseppe Liborio, published by Simon and Schuster, 1978.
5. Wikipedia.org and secondary references.
6. Brian Gootee, Research Geologist, Arizona Geological Survey.